Pergamon

Geochimica et Cosmochimica Acta, Vol. 68, No. 22, pp. 4745-4763, 2004

0016-7037/04 $30.00 + .00

doi:10.1016/j.gca.2004.05.022

Trapped Xe and I-Xe ages in aqueously altered CV3 meteorites

CHARLES M. HOHENBERG,* OLGA V. PRAVDIVTSEVA, and ALEX P. MESHIK

Department of Physics and McDonnell Center for Space Sciences, Washington University, St. Louis, MO 63130, USA

(*Received February* 10, 2004; *accepted in revised form May* 5, 2004)

Abstract—Twenty-two dark inclusions (DIs) from Allende (18), Leoville (2), Vigarano (1) and Efremovka (1) were studied by the I-Xe method. All except two of these DIs (Vigarano 2226 and Leoville LV2) produce well-defined isochrons, and precise I-Xe ages. The Allende DIs formed a tight group about 1.6 Ma older than Shallowater (4.566 ± 0.002 Ga), about 5 Ma older than four previously studied Allende CAIs. Most of the dark inclusions require trapped Xe with less ^{129}Xe (or more ^{128}Xe) than conventional planetary Xe (well restricted in composition by Q-Xe or OC-Xe). Studies of an irradiated/unirradiated DI pair from Allende demonstrate that the ^{128}Xe/^{132}Xe ratio in trapped is normal planetary, so that a ^{129}Xe/^{132}Xe ratio below planetary seems to be required. Yet, this is not possible given constraints on ^{129}Xe evolution in the early solar system. Trends among all of the Allende DIs suggest that an intimate mixture of partially decayed iodine and Xe formed a pseudo trapped Xe component enriched in both ^{129}Xe and ^{127}I, and subsequently in ^{128}Xe after n-capture during reactor irradiation. Enrichment in radiogenic ^{129}Xe, but with a ^{129}Xe/^{127}I ratio less than that observed in the iodine host phase, places closure of this trapped mixture ≥13 Ma after precipitation of the major iodine-bearing phase. Because the I-Xe isochron is a mixing line between iodine-derived and trapped Xe (pseudo or not), I-Xe ages, given by the slope of this mixing line, are not compromised by the presence of pseudo trapped Xe, and the precision of the I-Xe ages is given by the statistics of the line fit. *Copyright © 2004 Elsevier Ltd*

1. INTRODUCTION

Primitive meteorites, in particular carbonaceous chondrites, are known for their high abundance of heavy noble gases with a uniform composition originally denoted AVCC (for *A*verage *V*alue *C*arbonaceous *C*hondrite; Pepin and Signer, 1965; Reynolds et al., 1978). Pepin and Signer (1965) and Marti (1967) associated this recurrent Xe isotope pattern observed in all Xe-rich meteorites with "planetary", following the two-component elemental pattern, "planetary" and "solar", proposed by Signer and Suess (1963). It has since become clear that, although planetary Xe may contain complex mixtures of several minor components, and subtle differences may exist (Ott, 2002), planetary Xe can be effectively described by Q-Xe (Lewis et al., 1975; Ott et al., 1981), OC-Xe (*O*rdinary *C*hondritic Xe, Lavielle and Marti, 1992), or P1 (Huss et al., 1996). Planetary Xe lies at the core of the I-Xe dating, generally being one of the two components of the mixing line that is the I-Xe isochron and usually referred to as "trapped" to distinguish it from Xe produced by in situ processes. In most cases trapped Xe has the expected isotopic composition of Q-Xe.

The trapped Xe compositions have been observed to differ from planetary in two situations. Enstatite chondrites sometimes contain trapped Xe with a slightly enhanced ^{129}Xe. These were interpreted as evidence for closed system evolution in an environment with an elevated I/Xe ratio, such as might be found within the enstatite parent body (Kennedy, 1981; Kennedy et al., 1988). Arapahoe (L5) seemed to contain an apparent trapped composition depleted in ^{129}Xe and an abnormally old apparent I-Xe age, but the quality of the apparent isochron was rather poor (Drozd and Podosek, 1976). Subsequent experiments with artificially shocked samples of Bjurböle (Caffee et al., 1982) indicated that the "subplanetary"[1] nature of the trapped Xe in Arapahoe was most likely an artifact of shock, as was its apparent I-Xe age. Shock can disturb both trapped compositions and the slopes of apparent isochrons, as was demonstrated by the artificially shocked samples of Bjurböle. In these experiments, the resulting "isochrons" were poorly defined, most likely since shock-induced mobility depends more upon the compressibility of the host mineral than its thermal properties. There are cases where apparent "subplanetary" trapped Xe is probably not due to shock or to experimental artifacts (Swindle, 1998), but these have rather large statistical uncertainties.

Because Xe and iodine were present in the primitive solar system with about equal abundance (^{129}Xe/^{127}I ~ 1.4, Anders and Grevesse, 1989), and the initial ^{129}I/^{127}I ratio was ~10^{-4}, ^{129}Xe in the trapped component could not have evolved significantly over time due to the decay of ^{129}I, an observation also made by Gilmour and Saxton (2001). Therefore, ^{129}I decay can neither alter the ^{129}Xe/^{132}Xe ratio in an open system nor be responsible for a trapped Xe composition that is "subplanetary."

This work explores the composition of trapped Xe in 22 dark inclusions from Allende (18), Efremovka (1), Vigarano (1), and Leoville (2). Although most of these samples require "subplanetary" trapped Xe, the qualities of the isochrons are sufficiently good that they must be true two-component mixing lines between iodine-derived Xe and anomalous trapped Xe, not shock-

* Author to whom correspondence should be addressed (cmh@wustl.edu).

[1] "Subplanetary" trapped Xe refers to those cases when the I-Xe isochron passes below planetary. Although, in these cases, the position of the lower end-member is not known, if the ^{128}Xe/^{132}Xe ratio is assumed to be planetary, the ^{129}Xe/^{132}Xe ratio is lower than Q-Xe, or "subplanetary."

induced artifacts. The precision of the isochrons constrains the compositions of the trapped Xe and provides a unique opportunity to study its nature. Because the slope of the isochron alone establishes the ^{129*}Xe/^{128*}Xe ratio, and hence the I-Xe age, the validity of the I-Xe ages is not in question but the nature of "subplanetary" trapped Xe can be explored and its relation to aqueous alteration addressed.

2. ANALYTICAL PROCEDURE

Dark inclusions are lithic clasts commonly observed in the oxidized and reduced subgroups of the CV chondrites (Johnson et al., 1990). Fine-grained DIs including the ones discussed here were previously described (Fruland et al., 1978; Kracher et al., 1985; Bischoff et al., 1988; Johnson et al., 1990; Kojima et al., 1993; Kojima and Tomeoka, 1996; Weisberg et al., 1996; Buchanan et al., 1997; Brearley, 1998; Krot et al., 1998a; Krot et al., 1998b; Krot et al., 1999; Swindle et al., 1998). The mineralogy and petrology of the CV DIs indicate that they have experienced different types and degrees of alteration in an asteroidal setting before subsequent excavation and incorporation into their host meteorites (Kojima and Tomeoka, 1996; Krot et al., 1998a). Although the idea of alteration in asteroidal setting has recently become widely accepted, some authors favor a nebular alteration scenario (Palme et al., 1989; Kurat et al., 1989; Weisberg and Prinz, 1997).

The particular set of dark inclusions discussed here was chosen and analyzed with the intention of exploring the effects of aqueous alteration in reduced and oxidized CVs on their I-Xe systems, with possible application of the age information for the timing and location of the alteration events. Although some of these I-Xe ages have appeared in press (Pravdivtseva et al., 2003b; Pravdivtseva et al., 2003c), and will be discussed in more detail elsewhere, this work includes the data itself and concentrates on the implications of the anomalous trapped components.

For these I-Xe studies, material was selected from the central areas of each of the DI, avoiding the rims. Three DIs, Vigarano 2226, Allende 4884-6 and 4294-1, consisted of several fine grain clumps, whereas all of the other DIs were analyzed as single solid fragments. The DIs samples were loaded into individual fused quartz ampoules, sealed under vacuum, and arranged around the rim of an aluminum capsule and confined within 5 mm to a single horizontal plane. The capsule was then irradiated at the University of Missouri Research Reactor (MURR), designated SLC-14, receiving a total fluence of $\sim 2 \times 10^{19}$ neutrons/cm^2. The capsule was continuously rotated around the axis of the sample plane, and Co-doped Al flux wires were placed around the perimeter of the sample plane and at the middle of the irradiation package to monitor uniformity of the irradiation. The actual thermal fluence was uniform to $<1.0\%$ for each flux wire in the sample plane and differed by $\approx 2.5\%$ for points 5 cm above the sample plane (1% corresponds to an age uncertainty of $\sim$200,000 yr; for ± 5 mm, the actual vertical spread of the samples, the flux variation is negligible). The capsule was perforated at the top and bottom to allow pool water inside for thermal control. Two samples of the Shallowater reference were included in the irradiation as internal standards (Nichols et al., 1994).

After irradiation, the samples were weighed, transferred into the Pt boats, and loaded into the sample system of the mass spectrometer. Xenon was extracted by stepwise pyrolysis in a low blank coil. Use of the open coil for progressive heating of some samples greatly reduces the blank but does not allow accurate temperature determinations. Other samples were heated in an open coil with a radiation shield, which does provide accurate measure of the extraction temperatures. The released gases were cleaned by exposure to the hot getter pellets (SAES, ST-707, kept at 280°C) and, sequentially, to three freshly deposited Ti-film getters. Xe was then separated from the other noble gases by adsorption onto activated charcoal, maintained at -78°C by a mixture of CO_2-ice and methanol. Finally, the isotopic compositions of Xe at each extraction step were measured by ion counting mass spectrometry (Hohenberg, 1980). Both cold and hot (1500°) procedural blanks were routinely measured (both typically $\sim 1.2 \times 10^{-15}$ cm^3 STP ^{132}Xe and $\sim$ atmospheric in composition). To "clean" the coil of Pt (for thermal control) and contamination (for blanks), the coil was kept at $\sim$2000°C for 10 min after the melting of each sample and new hot blanks were measured before analyzing each new sample.

Xe data for these samples are presented in Table 1. The actual temperatures of DIs during stepwise heating can be as much as 200°C lower (for the bare coils) than that indicated by optical pyrometer calibration due to variable thermal coupling with the coil. The indicated temperatures can be approximately corrected for this effect by noting when the platinum foil melts, but only apparent temperatures are shown in the table. Samples analyzed with the radiation shield are inherently better thermally calibrated. However, regardless of temperature differences between different sets of samples, for each given sample the temperature steps are monotonic increments of known size.

3. RESULTS

In I-Xe dating, 15.7 Ma ^{129}I β–decays into ^{129*}Xe, providing a record of the parent nucleus (Reynolds, 1960). The analytical technique of I-Xe dating involves neutron irradiation, which converts a fraction of stable ^{127}I to ^{128*}Xe [^{127}I (n, $\gamma\beta$) $\rightarrow$ ^{128*}Xe]. In stepwise pyrolysis, each temperature fraction contains different proportions of trapped and iodine-derived Xe. The ratio of ^{129}Xe to some other Xe isotope not produced in the irradiation (such as ^{130}Xe or ^{132}Xe) is then plotted against the ratio of ^{128}Xe to that same isotope for each temperature fraction. If the ^{128*}Xe and ^{129*}Xe are both derived from initial iodine of uniform isotopic composition, the data will define a straight line whose slope is proportional to the ^{129}I/^{127}I ratio at the time of closure (Hohenberg and Reynolds, 1969; Swindle and Podosek, 1988). The I-Xe isochron is thus a mixing line between trapped and iodine-derived Xe. The simplicity of this technique is further enhanced by including in the irradiation a meteorite standard of known age, so that the relative I-Xe age Δt is given by the relative slopes of the isochrons, independent of flux monitors.

$$\frac{\left(\frac{^{129}I}{^{127}I}\right)_{sample}}{\left(\frac{^{129}I}{^{127}I}\right)_{Shallowater}} = e^{-\frac{\Delta t}{\tau}} \tag{1}$$

The uncertainty of the slope is provided statistically and can be further evaluated by the number of co-linear points and the corresponding χ-squared fit to the line. The use of a meteorite standard, to obtain the relative age, eliminates the necessity of determining the neutron capture probability of ^{127}I by using an absolute flux monitor such as KI, a technically difficult procedure given the large differences in iodine concentrations between the monitor and meteoritic minerals ($>10^9$:1; Hohenberg et al., 2000; Pravdivtseva et al., 2003a).

The resulting I-Xe ages Δt, relative to the Shallowater standard, are shown in Table 2 and Figure 1. These samples are so rich in radiogenic ^{129*}Xe (typically 3–4 $\times$ 10^{-10} cm^{3}STP/g, Table 2), and with procedural blanks three orders of magnitude lower, blanks do not contribute significantly, even in stepwise extractions. Moreover, the blanks are always similar in isotopic composition to trapped or atmospheric Xe. Even if they were more important, the presence of blank Xe would simply move the points along the isochron without significantly affecting the slope. Thus, while blank corrections are always evaluated, they seldom need to be applied.

The choice of ^{130}Xe or ^{132}Xe normalization is determined by the relative effects of corrections for spallation or fission con-

Table 1. Raw I-Xe data for dark inclusions from Allende, Vigarano, Efremovka, and Leoville.

Temp (°C)	$^{132}Xe \times 10^{-10}$ cm^3 STP/g	$^{132}Xe = 100$ ^{124}Xe	^{126}Xe	^{128}Xe	^{129}Xe	^{130}Xe	^{131}Xe	^{134}Xe	^{136}Xe
					Allende 4294-1				
800	0.1812	0.4317 ± 0.0259	0.4036 ± 0.0391	609.893 ± 2.594	110.34 ± 0.62	15.720 ± 0.160	424.966 ± 1.597	38.388 ± 0.342	32.892 ± 0.411
1000	0.6891	0.4900 ± 0.0198	0.4328 ± 0.0170	348.627 ± 0.986	113.63 ± 0.38	15.953 ± 0.112	310.529 ± 0.861	42.989 ± 0.244	39.526 ± 0.223
1100	0.09812	0.4346 ± 0.0521	0.4441 ± 0.0418	251.749 ± 1.531	119.29 ± 0.94	16.176 ± 0.244	360.793 ± 2.717	42.236 ± 0.721	39.473 ± 0.482
1150	0.2569	0.5729 ± 0.0256	0.4619 ± 0.0229	248.902 ± 0.999	129.74 ± 0.54	15.937 ± 0.223	336.484 ± 1.862	44.101 ± 0.427	40.719 ± 0.352
1200	0.5172	0.5405 ± 0.0218	0.4336 ± 0.0219	199.732 ± 0.755	186.76 ± 0.55	16.089 ± 0.166	202.040 ± 0.833	43.842 ± 0.296	40.276 ± 0.267
1250	0.04884	0.5323 ± 0.0667	0.4225 ± 0.0630	278.196 ± 1.604	278.10 ± 2.07	16.150 ± 0.357	133.289 ± 1.303	39.311 ± 0.554	36.503 ± 0.591
1300	2.575	0.4441 ± 0.0088	0.4256 ± 0.0091	222.646 ± 0.326	247.34 ± 0.39	16.275 ± 0.085	103.831 ± 0.250	38.491 ± 0.127	32.728 ± 0.090
1350	3.435	0.4496 ± 0.0084	0.4148 ± 0.0066	81.134 ± 0.121	149.31 ± 0.17	16.166 ± 0.052	99.134 ± 0.142	38.207 ± 0.093	32.588 ± 0.058
1400	3.199	0.4640 ± 0.0038	0.4227 ± 0.0066	56.851 ± 0.104	137.68 ± 0.14	16.246 ± 0.042	90.892 ± 0.181	38.425 ± 0.095	32.679 ± 0.078
1450	3.059	0.4507 ± 0.0069	0.4005 ± 0.0098	78.684 ± 0.143	160.31 ± 0.24	16.292 ± 0.068	86.962 ± 0.138	38.960 ± 0.090	33.392 ± 0.089
1500	0.08033	0.5447 ± 0.0541	0.4851 ± 0.0460	124.838 ± 0.693	195.46 ± 1.22	16.010 ± 0.293	91.833 ± 1.094	39.746 ± 0.584	36.166 ± 0.697
1600	0.04895	0.4209 ± 0.0673	0.4989 ± 0.0533	158.066 ± 1.477	217.76 ± 2.31	15.864 ± 0.457	96.869 ± 1.455	40.581 ± 0.832	37.478 ± 0.720
1700	0.01241	0.3905 ± 0.1038	0.3895 ± 0.1125	158.222 ± 2.336	217.00 ± 4.67	14.045 ± 0.720	111.835 ± 2.329	45.898 ± 1.778	41.594 ± 2.045
Total	17.64	0.4583 ± 0.0032	0.4182 ± 0.0033	120.770 ± 0.097	163.14 ± 0.09	16.201 ± 0.025	115.832 ± 0.093	38.894 ± 0.042	33.452 ± 0.033
					Allende 4301-1				
800	0.1040	0.3910 ± 0.0402	0.4673 ± 0.0388	1401.632 ± 6.338	112.65 ± 0.84	16.384 ± 0.185	373.486 ± 2.226	38.521 ± 0.332	32.863 ± 0.270
1000	1.393	0.5344 ± 0.0102	0.4623 ± 0.0128	247.270 ± 0.678	112.49 ± 0.19	16.004 ± 0.054	150.382 ± 0.209	44.045 ± 0.072	41.210 ± 0.094
1100	0.1494	0.5313 ± 0.0349	0.4663 ± 0.0323	58.848 ± 0.517	114.68 ± 0.79	15.940 ± 0.100	90.041 ± 0.359	40.935 ± 0.321	36.390 ± 0.196
1200	1.063	0.4645 ± 0.0123	0.4342 ± 0.0126	49.929 ± 0.139	118.37 ± 0.21	16.200 ± 0.048	87.883 ± 0.131	38.657 ± 0.078	32.894 ± 0.073
1300	2.282	0.4592 ± 0.0080	0.4082 ± 0.0078	30.874 ± 0.044	112.29 ± 0.14	16.188 ± 0.046	84.698 ± 0.130	38.125 ± 0.058	32.117 ± 0.080
1350	2.540	0.4629 ± 0.0086	0.4162 ± 0.0083	37.576 ± 0.073	119.15 ± 0.14	16.143 ± 0.043	84.371 ± 0.119	38.112 ± 0.051	32.060 ± 0.048
1400	3.188	0.4658 ± 0.0068	0.3970 ± 0.0075	53.717 ± 0.057	133.47 ± 0.11	16.160 ± 0.041	86.027 ± 0.091	38.307 ± 0.060	32.270 ± 0.071
1450	1.207	0.4507 ± 0.0105	0.4081 ± 0.0091	56.536 ± 0.137	137.99 ± 0.26	16.191 ± 0.071	86.355 ± 0.161	38.503 ± 0.091	32.525 ± 0.075
1500	1.124	0.4353 ± 0.0115	0.4204 ± 0.0130	75.518 ± 0.116	154.27 ± 0.19	16.270 ± 0.052	87.044 ± 0.156	38.343 ± 0.083	32.642 ± 0.072
1600	1.099	0.4765 ± 0.0092	0.3965 ± 0.0107	105.253 ± 0.158	178.95 ± 0.23	16.161 ± 0.048	88.896 ± 0.129	38.685 ± 0.097	32.864 ± 0.088
1700	0.3929	0.4413 ± 0.0194	0.4105 ± 0.0228	119.322 ± 0.238	193.52 ± 0.33	16.252 ± 0.085	89.557 ± 0.266	38.904 ± 0.135	33.212 ± 0.114
1800	0.1834	0.5308 ± 0.0310	0.4020 ± 0.0231	112.242 ± 0.414	188.92 ± 0.51	16.267 ± 0.148	90.062 ± 0.317	39.198 ± 0.259	33.625 ± 0.179
1900	0.2052	0.5498 ± 0.0184	0.4571 ± 0.0310	99.868 ± 0.317	179.72 ± 0.55	16.331 ± 0.103	88.146 ± 0.340	38.825 ± 0.214	33.318 ± 0.217
2000	0.00278	0.5154 ± 0.0617	0.3231 ± 0.0581	76.181 ± 0.665	159.85 ± 1.45	16.409 ± 0.276	85.018 ± 0.806	39.209 ± 0.546	33.011 ± 0.565
Total	14.96	0.4694 ± 0.0032	0.4156 ± 0.0033	83.432 ± 0.564	132.66 ± 0.10	16.166 ± 0.017	94.188 ± 0.169	38.915 ± 0.028	33.282 ± 0.033
					Allende 4314-3				
800	0.1192	0.4738 ± 0.0392	0.4593 ± 0.0538	1102.442 ± 6.447	120.94 ± 1.10	16.230 ± 0.318	354.845 ± 1.730	38.227 ± 0.220	32.904 ± 0.250
1000	1.044	0.5972 ± 0.0140	0.4744 ± 0.0127	227.460 ± 0.287	108.54 ± 0.23	15.926 ± 0.053	121.331 ± 0.242	46.558 ± 0.107	45.178 ± 0.080
1100	0.8724	0.4610 ± 0.0145	0.4474 ± 0.0138	107.081 ± 0.175	110.02 ± 0.18	16.208 ± 0.046	105.841 ± 0.169	38.425 ± 0.090	32.380 ± 0.093
1200	1.422	0.4451 ± 0.0095	0.4248 ± 0.0128	44.347 ± 0.083	110.73 ± 0.14	16.199 ± 0.040	86.207 ± 0.131	38.183 ± 0.075	32.047 ± 0.071
1300	2.927	0.4654 ± 0.0072	0.4280 ± 0.0075	40.490 ± 0.050	113.38 ± 0.12	16.237 ± 0.026	85.492 ± 0.078	38.193 ± 0.049	32.091 ± 0.048
1350	3.191	0.4654 ± 0.0075	0.4179 ± 0.0058	46.328 ± 0.054	123.26 ± 0.11	16.160 ± 0.040	86.207 ± 0.101	38.267 ± 0.046	32.147 ± 0.047
1400	2.760	0.4603 ± 0.0057	0.4169 ± 0.0050	49.292 ± 0.072	130.92 ± 0.16	16.207 ± 0.038	85.997 ± 0.098	38.301 ± 0.057	32.258 ± 0.064
1450	1.066	0.4631 ± 0.0119	0.3980 ± 0.0130	60.033 ± 0.146	141.41 ± 0.20	16.207 ± 0.047	87.102 ± 0.171	38.311 ± 0.094	32.495 ± 0.062
1500	0.4247	0.4810 ± 0.0209	0.4268 ± 0.0176	80.831 ± 0.208	159.90 ± 0.45	16.321 ± 0.070	89.986 ± 0.204	39.003 ± 0.133	33.189 ± 0.119
1600	0.4496	0.5287 ± 0.0264	0.4181 ± 0.0180	103.697 ± 0.246	178.91 ± 0.38	16.118 ± 0.051	90.582 ± 0.270	38.954 ± 0.121	33.045 ± 0.105
1700	0.2560	0.4461 ± 0.0259	0.4191 ± 0.0291	118.465 ± 0.343	192.01 ± 0.44	16.064 ± 0.085	92.014 ± 0.368	39.181 ± 0.240	33.324 ± 0.177
1800	0.1050	0.5357 ± 0.1058	0.3733 ± 0.0277	123.282 ± 0.507	194.29 ± 0.61	16.042 ± 0.170	94.171 ± 0.493	39.266 ± 0.241	33.805 ± 0.235
1900	0.02163	0.4712 ± 0.1176	0.4878 ± 0.0998	126.596 ± 1.458	194.08 ± 1.63	15.831 ± 0.379	95.067 ± 0.872	39.478 ± 0.619	33.082 ± 0.460
2000	0.00847	−0.3520 ± 0.1004	0.1543 ± 0.1594	93.873 ± 3.459	163.85 ± 4.61	14.143 ± 1.018	83.992 ± 2.813	35.485 ± 1.932	28.571 ± 1.791
Total	14.67	0.4736 ± 0.0033	0.4250 ± 0.0031	79.712 ± 0.298	125.58 ± 0.06	16.177 ± 0.015	92.355 ± 0.072	38.919 ± 0.025	33.209 ± 0.027

Table 1. (Continued)

Temp (°C)	^{132}Xe × 10^{-10} cm^3 STP/g	^{132}Xe = 100							
		^{124}Xe	^{126}Xe	^{128}Xe	^{129}Xe	^{130}Xe	^{131}Xe	^{134}Xe	^{136}Xe
				Allende 4320-1					
800	0.1527	0.4810 ± 0.0641	0.3821 ± 0.0605	891.416 ± 5.957	108.33 ± 0.92	16.024 ± 0.312	209.199 ± 2.147	37.781 ± 0.673	32.581 ± 0.765
1000	1.835	0.5165 ± 0.0200	0.4704 ± 0.0136	203.340 ± 0.443	108.81 ± 0.44	16.013 ± 0.152	129.005 ± 0.494	44.541 ± 0.267	42.085 ± 0.237
1100	4.775	0.4722 ± 0.0123	0.4326 ± 0.0114	26.516 ± 0.125	107.89 ± 0.20	16.284 ± 0.105	84.838 ± 0.303	39.189 ± 0.154	33.825 ± 0.174
1150	8.269	0.4740 ± 0.0074	0.4259 ± 0.0089	18.573 ± 0.079	108.39 ± 0.23	16.232 ± 0.085	82.776 ± 0.172	38.036 ± 0.114	32.125 ± 0.094
1200	6.313	0.4539 ± 0.0070	0.4128 ± 0.0082	22.403 ± 0.068	113.05 ± 0.18	16.387 ± 0.075	83.612 ± 0.165	37.912 ± 0.092	32.121 ± 0.109
1250	4.169	0.4621 ± 0.0103	0.4058 ± 0.0115	39.023 ± 0.126	126.39 ± 0.29	16.236 ± 0.080	84.165 ± 0.281	38.517 ± 0.138	32.522 ± 0.166
1300	2.225	0.4850 ± 0.0175	0.4440 ± 0.0165	51.753 ± 0.167	139.01 ± 0.37	16.134 ± 0.146	84.305 ± 0.292	38.078 ± 0.250	32.377 ± 0.170
1350	1.209	0.4780 ± 0.0227	0.4217 ± 0.0204	75.804 ± 0.330	159.26 ± 0.53	16.429 ± 0.156	85.689 ± 0.326	38.227 ± 0.334	33.395 ± 0.242
1400	0.4943	0.4483 ± 0.0317	0.3768 ± 0.0380	99.574 ± 0.533	181.81 ± 0.94	16.415 ± 0.274	86.710 ± 0.518	38.628 ± 0.484	33.740 ± 0.357
1450	0.1120	0.5210 ± 0.0727	0.4599 ± 0.0676	100.561 ± 1.190	182.88 ± 1.75	16.736 ± 0.493	88.354 ± 1.313	37.525 ± 0.818	33.307 ± 0.866
1500	0.04427	0.4526 ± 0.1506	0.5468 ± 0.1205	106.230 ± 2.728	188.49 ± 3.82	16.088 ± 0.730	101.149 ± 2.357	39.947 ± 1.596	32.425 ± 1.393
1600	0.02449	0.6910 ± 0.2059	0.2785 ± 0.1349	96.686 ± 2.792	174.43 ± 4.49	16.514 ± 1.025	102.908 ± 3.434	35.820 ± 1.686	30.083 ± 1.692
1700	0.02656	0.6069 ± 0.1712	0.3525 ± 0.1493	95.400 ± 1.605	165.24 ± 3.82	15.486 ± 0.809	99.321 ± 3.464	37.767 ± 1.735	32.248 ± 2.069
Total	29.65	0.4714 ± 0.0041	0.4244 ± 0.0043	46.220 ± 0.076	117.96 ± 0.10	16.264 ± 0.039	87.372 ± 0.097	38.684 ± 0.057	33.173 ± 0.056
				Allende 4884-1					
800	0.3364	0.4757 ± 0.0262	0.4094 ± 0.0276	113.052 ± 0.626	111.24 ± 0.58	16.157 ± 0.199	280.305 ± 1.521	38.810 ± 0.336	33.347 ± 0.311
1000	1.040	0.5551 ± 0.0170	0.4420 ± 0.0111	34.054 ± 0.142	110.52 ± 0.33	16.164 ± 0.096	113.695 ± 0.453	43.441 ± 0.164	40.549 ± 0.179
1100	2.268	0.4867 ± 0.0073	0.4185 ± 0.0085	17.692 ± 0.071	109.93 ± 0.19	16.101 ± 0.108	86.803 ± 0.147	39.822 ± 0.155	34.358 ± 0.111
1150	3.141	0.4660 ± 0.0100	0.4220 ± 0.0105	16.588 ± 0.061	109.80 ± 0.16	16.257 ± 0.053	83.977 ± 0.186	38.376 ± 0.106	32.332 ± 0.121
1200	3.339	0.4596 ± 0.0094	0.4242 ± 0.0084	24.468 ± 0.053	116.81 ± 0.12	16.327 ± 0.072	85.717 ± 0.125	38.142 ± 0.137	32.299 ± 0.106
1250	1.768	0.4822 ± 0.0129	0.4158 ± 0.0142	39.142 ± 0.098	129.55 ± 0.34	16.504 ± 0.078	88.206 ± 0.172	38.531 ± 0.162	32.485 ± 0.137
1300	1.831	0.4593 ± 0.0128	0.4258 ± 0.0074	57.491 ± 0.127	145.75 ± 0.28	16.336 ± 0.089	89.127 ± 0.249	38.151 ± 0.115	32.718 ± 0.130
1350	1.275	0.4766 ± 0.0137	0.4074 ± 0.0132	85.678 ± 0.176	170.72 ± 0.31	16.014 ± 0.109	90.202 ± 0.373	38.801 ± 0.150	32.991 ± 0.181
1400	0.7135	0.4841 ± 0.0197	0.4010 ± 0.0147	103.930 ± 0.501	187.66 ± 0.45	15.965 ± 0.112	90.113 ± 0.412	38.952 ± 0.284	33.382 ± 0.228
1450	0.2070	0.4529 ± 0.0283	0.3965 ± 0.0252	106.617 ± 0.532	187.36 ± 0.79	15.887 ± 0.228	88.395 ± 0.458	37.922 ± 0.375	33.091 ± 0.372
1500	0.1558	0.4702 ± 0.0372	0.3620 ± 0.0411	107.156 ± 0.718	191.13 ± 1.26	16.049 ± 0.299	89.430 ± 0.897	38.671 ± 0.558	33.101 ± 0.538
1600	0.1308	0.4753 ± 0.0381	0.3721 ± 0.0430	108.090 ± 1.018	189.79 ± 1.31	16.748 ± 0.326	90.336 ± 0.796	38.471 ± 0.572	33.425 ± 0.307
1700	0.03541	0.4200 ± 0.0724	0.5369 ± 0.0642	102.277 ± 1.358	188.90 ± 7.72	16.108 ± 0.470	96.352 ± 1.422	37.131 ± 1.071	32.871 ± 1.221
Total	16.24	0.4760 ± 0.0040	0.4196 ± 0.0038	40.746 ± 0.045	128.33 ± 0.08	16.242 ± 0.030	92.685 ± 0.084	38.908 ± 0.052	33.335 ± 0.047
				Allende 4884-2					
800	0.01165	0.5830 ± 0.3209	−0.1523 ± 0.2499	978.231 ± 26.322	141.72 ± 3.88	17.358 ± 1.425	595.492 ± 15.025	37.548 ± 2.580	29.421 ± 2.441
1000	0.1274	0.4276 ± 0.0663	0.3630 ± 0.0579	246.799 ± 1.820	143.28 ± 1.64	15.051 ± 0.402	456.606 ± 3.154	44.335 ± 0.753	42.529 ± 0.874
1100	0.1779	0.6427 ± 0.0688	0.4350 ± 0.0551	158.120 ± 1.160	184.70 ± 1.32	15.185 ± 0.329	248.589 ± 2.576	49.287 ± 0.630	49.600 ± 0.596
1150	0.1537	0.5899 ± 0.0510	0.4554 ± 0.0606	245.059 ± 1.841	276.25 ± 1.97	16.001 ± 0.354	142.398 ± 1.248	43.108 ± 0.644	40.510 ± 0.710
1200	0.3525	0.4730 ± 0.0405	0.4263 ± 0.0321	197.905 ± 1.085	250.96 ± 1.43	15.936 ± 0.226	112.613 ± 0.911	40.713 ± 0.436	35.232 ± 0.284
1250	0.3507	0.4672 ± 0.0336	0.3567 ± 0.0458	269.314 ± 1.182	318.28 ± 1.66	16.748 ± 0.296	118.951 ± 0.795	40.627 ± 0.457	37.057 ± 0.344
1300	0.3293	0.4966 ± 0.0313	0.3981 ± 0.0335	277.223 ± 1.195	327.15 ± 1.15	16.490 ± 0.254	116.350 ± 0.815	40.896 ± 0.387	36.615 ± 0.333
1350	0.4537	0.5641 ± 0.0354	0.4342 ± 0.0318	297.277 ± 1.480	349.61 ± 1.36	15.951 ± 0.219	108.618 ± 0.680	41.281 ± 0.414	36.933 ± 0.272
1400	0.3267	0.4194 ± 0.0438	0.4633 ± 0.0372	638.168 ± 3.302	646.71 ± 3.31	16.204 ± 0.314	132.500 ± 0.892	44.642 ± 0.569	41.702 ± 0.412
1450	0.001702	−1.6412 ± 0.9655	−2.8853 ± 0.8348	1035.167 ± 48.968	955.65 ± 49.34	14.182 ± 3.615	476.661 ± 35.050	53.240 ± 6.575	45.552 ± 4.604
1500	0.03300	0.8260 ± 0.1409	0.4653 ± 0.1335	964.693 ± 16.556	953.14 ± 12.13	15.486 ± 0.689	161.258 ± 4.573	49.534 ± 1.756	47.172 ± 1.755
1600	0.02250	0.1470 ± 0.1974	0.1768 ± 0.1176	814.616 ± 11.198	801.41 ± 14.69	16.185 ± 1.281	147.056 ± 3.367	47.128 ± 1.229	45.290 ± 1.502
1700	0.01835	0.2748 ± 0.2048	0.2997 ± 0.2064	792.736 ± 9.658	802.46 ± 12.51	17.228 ± 1.189	127.809 ± 4.076	46.427 ± 1.700	45.457 ± 1.866
Total	2.359	0.5028 ± 0.0151	0.4097 ± 0.0144	328.074 ± 0.805	355.55 ± 0.80	16.086 ± 0.100	150.606 ± 0.441	42.600 ± 0.176	39.062 ± 0.142

				Allende 4884-3					
800	0.1423	0.5091 ± 0.0590	0.4214 ± 0.0408	118.666 ± 0.794	108.25 ± 0.75	15.771 ± 0.282	190.957 ± 1.462	37.924 ± 0.505	31.484 ± 0.397
1000	0.9093	0.5411 ± 0.0186	0.4603 ± 0.0168	60.847 ± 0.221	113.18 ± 0.33	15.923 ± 0.145	146.021 ± 0.455	42.136 ± 0.226	37.998 ± 0.217
1100	2.235	0.5182 ± 0.0120	0.4430 ± 0.0111	24.098 ± 0.110	116.10 ± 0.22	16.135 ± 0.097	92.065 ± 0.273	42.300 ± 0.215	38.564 ± 0.137
1150	5.176	0.4762 ± 0.0056	0.4266 ± 0.0071	19.760 ± 0.052	115.00 ± 0.16	16.223 ± 0.077	84.633 ± 0.118	38.974 ± 0.069	33.178 ± 0.082
1200	8.728	0.4535 ± 0.0033	0.4181 ± 0.0077	26.684 ± 0.036	120.83 ± 0.12	16.321 ± 0.032	83.553 ± 0.108	38.102 ± 0.061	32.136 ± 0.088
1250	3.765	0.4608 ± 0.0065	0.4004 ± 0.0093	26.944 ± 0.065	120.05 ± 0.19	16.200 ± 0.041	84.089 ± 0.128	38.324 ± 0.100	32.201 ± 0.096
1300	4.578	0.4762 ± 0.0072	0.4202 ± 0.0070	42.496 ± 0.075	133.80 ± 0.12	16.243 ± 0.069	85.369 ± 0.115	38.315 ± 0.060	32.567 ± 0.094
1350	2.401	0.4736 ± 0.0121	0.3979 ± 0.0082	47.677 ± 0.098	138.00 ± 0.24	16.229 ± 0.070	85.330 ± 0.163	38.226 ± 0.170	32.395 ± 0.129
1400	0.6481	0.4429 ± 0.0205	0.4162 ± 0.0187	83.221 ± 0.303	168.59 ± 0.64	16.243 ± 0.156	88.272 ± 0.359	38.289 ± 0.385	32.830 ± 0.208
1450	0.1508	0.4883 ± 0.0382	0.3775 ± 0.0515	99.142 ± 0.732	185.75 ± 1.20	16.653 ± 0.254	91.663 ± 0.927	38.660 ± 0.619	34.424 ± 0.448
1500	0.09577	0.6164 ± 0.0489	0.4482 ± 0.0534	99.492 ± 0.967	183.87 ± 1.05	16.229 ± 0.375	91.353 ± 1.114	39.454 ± 0.511	33.229 ± 0.587
1600	0.09104	0.5206 ± 0.0528	0.4132 ± 0.0569	104.176 ± 1.237	186.36 ± 1.56	15.814 ± 0.400	92.316 ± 1.322	39.771 ± 0.894	33.376 ± 0.552
1700	0.01674	0.3423 ± 0.1228	0.1954 ± 0.1283	105.989 ± 1.586	192.88 ± 3.44	15.885 ± 1.018	107.421 ± 2.928	39.385 ± 1.286	36.120 ± 1.513
Total	28.94	0.4724 ± 0.0026	0.4189 ± 0.0034	33.223 ± 0.028	124.36 ± 0.07	16.236 ± 0.024	87.614 ± 0.056	38.799 ± 0.037	33.135 ± 0.040
				Allende 4884-5					
800	0.1969	0.4829 ± 0.0570	0.3883 ± 0.0517	127.744 ± 0.864	115.41 ± 0.64	15.806 ± 0.363	274.125 ± 1.786	38.853 ± 0.588	33.181 ± 0.596
1000	0.5237	0.4836 ± 0.0304	0.3391 ± 0.0171	67.351 ± 0.312	120.64 ± 0.66	15.693 ± 0.166	168.568 ± 0.842	41.070 ± 0.281	37.397 ± 0.330
1100	1.327	0.5102 ± 0.0089	0.4217 ± 0.0072	26.871 ± 0.066	115.64 ± 0.16	16.263 ± 0.045	93.247 ± 0.206	41.006 ± 0.081	36.506 ± 0.078
1150	2.102	0.4796 ± 0.0066	0.4160 ± 0.0067	22.715 ± 0.046	114.33 ± 0.12	16.223 ± 0.050	85.699 ± 0.129	39.171 ± 0.079	33.858 ± 0.076
1200	3.593	0.4741 ± 0.0042	0.4180 ± 0.0051	23.112 ± 0.036	115.75 ± 0.13	16.283 ± 0.041	84.447 ± 0.109	38.235 ± 0.063	32.390 ± 0.059
1250	1.825	0.4644 ± 0.0146	0.4109 ± 0.0131	38.256 ± 0.132	128.75 ± 0.25	16.254 ± 0.122	85.949 ± 0.290	38.420 ± 0.155	32.406 ± 0.172
1300	1.611	0.4605 ± 0.0127	0.4242 ± 0.0139	72.264 ± 0.252	157.74 ± 0.50	16.366 ± 0.138	87.166 ± 0.360	38.748 ± 0.174	32.975 ± 0.249
1350	1.671	0.4667 ± 0.0190	0.4049 ± 0.0143	96.434 ± 0.243	179.57 ± 0.54	16.333 ± 0.119	87.333 ± 0.364	38.474 ± 0.223	33.094 ± 0.186
1400	1.263	0.4767 ± 0.0160	0.4494 ± 0.0199	127.970 ± 0.453	207.02 ± 0.65	16.160 ± 0.118	89.513 ± 0.391	38.905 ± 0.243	33.299 ± 0.205
1450	0.3549	0.4949 ± 0.0263	0.5676 ± 0.0381	126.619 ± 0.716	205.82 ± 1.09	16.433 ± 0.182	92.025 ± 0.776	38.943 ± 0.553	33.279 ± 0.433
1500	0.2471	0.5168 ± 0.0406	0.4632 ± 0.0420	123.862 ± 0.642	203.79 ± 1.02	16.279 ± 0.264	91.724 ± 0.967	39.506 ± 0.489	33.272 ± 0.421
1600	0.05085	0.4857 ± 0.0817	0.4378 ± 0.0964	119.306 ± 1.851	199.36 ± 1.75	15.489 ± 0.639	101.011 ± 1.833	38.021 ± 1.085	33.091 ± 0.968
1800	0.08622	0.5098 ± 0.0520	0.3731 ± 0.0493	124.929 ± 1.135	204.24 ± 1.66	14.668 ± 0.464	95.173 ± 1.492	39.100 ± 0.954	33.593 ± 0.801
Total	14.85	0.4767 ± 0.0041	0.4200 ± 0.0039	55.774 ± 0.078	141.22 ± 0.12	16.238 ± 0.032	92.548 ± 0.097	38.928 ± 0.051	33.420 ± 0.052
				Allende 4884-6					
800	0.5467	0.3991 ± 0.0246	0.4255 ± 0.0160	88.633 ± 0.365	112.53 ± 0.46	15.901 ± 0.196	233.208 ± 0.855	38.952 ± 0.219	32.727 ± 0.275
1000	1.024	0.5288 ± 0.0148	0.4492 ± 0.0188	42.541 ± 0.154	113.61 ± 0.21	16.204 ± 0.152	103.482 ± 0.436	42.732 ± 0.219	39.204 ± 0.263
1100	4.487	0.5120 ± 0.0078	0.4129 ± 0.0078	19.165 ± 0.048	110.45 ± 0.17	16.394 ± 0.040	84.565 ± 0.190	40.371 ± 0.116	35.295 ± 0.075
1150	7.265	0.4758 ± 0.0076	0.4138 ± 0.0075	17.288 ± 0.034	110.97 ± 0.11	16.197 ± 0.045	83.257 ± 0.120	38.288 ± 0.064	32.433 ± 0.085
1200	7.112	0.4770 ± 0.0093	0.4090 ± 0.0068	18.535 ± 0.046	112.26 ± 0.12	16.346 ± 0.051	83.349 ± 0.116	38.108 ± 0.076	32.045 ± 0.075
1250	3.336	0.4610 ± 0.0076	0.4059 ± 0.0084	42.920 ± 0.107	133.36 ± 0.26	16.366 ± 0.084	85.641 ± 0.146	38.220 ± 0.138	32.553 ± 0.124
1300	3.299	0.4607 ± 0.0100	0.4014 ± 0.0107	44.273 ± 0.093	134.47 ± 0.14	16.278 ± 0.080	85.254 ± 0.152	38.149 ± 0.085	32.518 ± 0.108
1350	1.726	0.4878 ± 0.0163	0.4260 ± 0.0125	69.716 ± 0.194	157.53 ± 0.36	16.400 ± 0.116	86.395 ± 0.266	38.769 ± 0.137	33.095 ± 0.132
1400	0.9521	0.5094 ± 0.0235	0.4081 ± 0.0185	91.826 ± 0.279	176.52 ± 0.38	16.251 ± 0.094	86.489 ± 0.309	38.346 ± 0.202	32.648 ± 0.233
1450	0.2287	0.4755 ± 0.0474	0.4471 ± 0.0373	94.147 ± 0.597	179.32 ± 1.24	15.789 ± 0.146	89.281 ± 0.689	39.565 ± 0.466	33.525 ± 0.415
1500	0.08871	0.5919 ± 0.0504	0.4278 ± 0.0743	97.115 ± 1.215	183.31 ± 1.87	16.233 ± 0.419	92.019 ± 1.110	38.510 ± 0.508	33.112 ± 0.718
1600	0.08012	0.4414 ± 0.0728	0.3923 ± 0.0531	100.565 ± 0.983	184.18 ± 1.05	15.617 ± 0.371	92.137 ± 1.467	38.642 ± 0.884	31.598 ± 0.774
1700	0.04079	0.5052 ± 0.0729	0.2702 ± 0.0860	108.147 ± 1.733	188.29 ± 2.42	16.352 ± 0.622	97.542 ± 1.843	39.299 ± 0.902	33.379 ± 1.256
Total	30.22	0.4806 ± 0.0037	0.4123 ± 0.0033	32.313 ± 0.030	122.13 ± 0.07	16.293 ± 0.024	87.750 ± 0.062	38.737 ± 0.037	33.078 ± 0.038

Table 1. (Continued)

Temp (°C)	$^{132}Xe \times 10^{-10}$ cm^3 STP/g	$^{132}Xe = 100$							
		^{124}Xe	^{126}Xe	^{128}Xe	^{129}Xe	^{130}Xe	^{131}Xe	^{134}Xe	^{136}Xe
					Allende IV-I				
800	0.05225	0.3184 ± 0.0442	0.3228 ± 0.0509	250.346 ± 1.198	102.40 ± 0.44	15.177 ± 0.154	148.409 ± 0.628	38.634 ± 0.243	32.455 ± 0.251
1000	0.3289	0.4821 ± 0.0199	0.4358 ± 0.0174	223.389 ± 0.461	113.47 ± 0.24	15.866 ± 0.072	230.138 ± 0.501	41.578 ± 0.139	37.302 ± 0.145
1100	0.2954	0.5245 ± 0.0229	0.4458 ± 0.0201	105.299 ± 0.181	114.31 ± 0.26	15.877 ± 0.104	134.397 ± 0.244	44.060 ± 0.122	41.588 ± 0.131
1200	0.8578	0.5262 ± 0.0120	0.4337 ± 0.0085	55.281 ± 0.125	115.99 ± 0.25	16.095 ± 0.052	108.161 ± 0.185	42.479 ± 0.086	38.746 ± 0.082
1300	1.308	0.4654 ± 0.0072	0.4147 ± 0.0090	29.686 ± 0.042	113.72 ± 0.12	16.154 ± 0.032	85.909 ± 0.119	38.240 ± 0.065	32.237 ± 0.074
1350	1.347	0.4581 ± 0.0081	0.4112 ± 0.0089	28.932 ± 0.046	114.93 ± 0.14	16.123 ± 0.035	84.896 ± 0.134	38.004 ± 0.066	31.972 ± 0.052
1400	2.542	0.4590 ± 0.0054	0.4145 ± 0.0074	40.510 ± 0.049	124.91 ± 0.10	16.111 ± 0.025	86.621 ± 0.083	38.124 ± 0.037	32.136 ± 0.035
1450	1.592	0.4739 ± 0.0070	0.4078 ± 0.0061	58.721 ± 0.081	141.65 ± 0.19	16.197 ± 0.032	89.293 ± 0.094	38.453 ± 0.051	32.480 ± 0.053
1500	1.464	0.4575 ± 0.0074	0.3913 ± 0.0077	52.674 ± 0.067	138.61 ± 0.16	16.146 ± 0.034	87.247 ± 0.094	38.303 ± 0.067	32.425 ± 0.060
1550	1.020	0.4958 ± 0.0206	0.4453 ± 0.0228	66.257 ± 0.232	150.54 ± 0.34	16.263 ± 0.071	89.011 ± 0.283	38.663 ± 0.146	32.628 ± 0.135
1600	0.4424	0.4644 ± 0.0151	0.3937 ± 0.0153	82.474 ± 0.170	164.98 ± 0.28	16.269 ± 0.045	91.461 ± 0.201	38.635 ± 0.104	33.019 ± 0.089
1700	0.3820	0.5412 ± 0.0279	0.4601 ± 0.0259	91.936 ± 0.448	173.31 ± 0.50	16.171 ± 0.143	92.951 ± 0.334	38.713 ± 0.215	32.758 ± 0.223
1800	0.1665	0.4500 ± 0.0196	0.4177 ± 0.0229	106.891 ± 0.253	186.67 ± 0.46	16.321 ± 0.096	95.701 ± 0.326	39.212 ± 0.197	33.328 ± 0.188
1900	0.0601	0.4594 ± 0.0538	0.4205 ± 0.0429	117.564 ± 0.371	195.84 ± 0.77	16.213 ± 0.115	97.372 ± 0.563	38.899 ± 0.333	32.879 ± 0.185
Total	11.86	0.4738 ± 0.0032	0.4162 ± 0.0035	57.386 ± 0.113	131.64 ± 0.07	16.140 ± 0.013	94.555 ± 0.098	38.854 ± 0.025	33.184 ± 0.024
					Allende IV-2				
800	0.01075	0.3589 ± 0.1936	0.2728 ± 0.1937	262.768 ± 5.334	120.27 ± 4.32	16.477 ± 0.926	381.068 ± 8.696	40.697 ± 1.849	31.867 ± 1.781
1000	0.1781	0.5358 ± 0.0777	0.4040 ± 0.0733	189.876 ± 1.143	117.98 ± 0.86	16.029 ± 0.287	381.749 ± 2.722	38.905 ± 0.524	32.677 ± 0.289
1100	0.1688	0.4454 ± 0.0683	0.3907 ± 0.0586	104.576 ± 0.616	119.79 ± 0.88	15.951 ± 0.283	159.350 ± 1.148	38.680 ± 0.393	33.056 ± 0.301
1200	0.3252	0.4694 ± 0.0430	0.4520 ± 0.0492	71.309 ± 0.368	120.56 ± 0.65	15.774 ± 0.217	135.859 ± 0.549	41.826 ± 0.379	37.792 ± 0.218
1300	0.8849	0.4878 ± 0.0243	0.4114 ± 0.0196	46.823 ± 0.245	125.61 ± 0.38	16.028 ± 0.128	90.335 ± 0.312	42.551 ± 0.154	38.452 ± 0.156
1350	1.569	0.5382 ± 0.0181	0.4409 ± 0.0182	34.211 ± 0.147	120.62 ± 0.33	16.038 ± 0.086	84.962 ± 0.305	40.323 ± 0.124	35.253 ± 0.149
1400	3.236	0.4573 ± 0.0115	0.4131 ± 0.0143	24.369 ± 0.091	115.06 ± 0.25	16.056 ± 0.063	83.907 ± 0.183	38.357 ± 0.147	32.381 ± 0.129
1450	2.951	0.4560 ± 0.0114	0.4060 ± 0.0149	23.974 ± 0.091	115.74 ± 0.24	16.288 ± 0.062	83.797 ± 0.178	37.917 ± 0.095	32.101 ± 0.099
1550	2.811	0.4586 ± 0.0169	0.4246 ± 0.0167	43.894 ± 0.114	132.24 ± 0.30	16.132 ± 0.060	89.153 ± 0.221	38.379 ± 0.125	32.555 ± 0.097
1700	1.370	0.4800 ± 0.0232	0.3664 ± 0.0202	73.378 ± 0.189	158.72 ± 0.40	16.233 ± 0.100	92.142 ± 0.300	38.587 ± 0.137	32.848 ± 0.111
1800	0.4340	0.4835 ± 0.0315	0.4198 ± 0.0421	98.958 ± 0.398	181.64 ± 0.60	16.235 ± 0.175	91.252 ± 0.412	38.793 ± 0.307	32.957 ± 0.301
1900	0.07184	0.4512 ± 0.0739	0.4081 ± 0.0827	97.581 ± 0.973	180.91 ± 1.76	16.333 ± 0.454	88.670 ± 1.267	38.971 ± 0.790	32.396 ± 0.640
Total	14.01	0.4723 ± 0.0063	0.4129 ± 0.0068	42.546 ± 0.156	126.84 ± 0.15	16.133 ± 0.029	92.647 ± 0.174	38.886 ± 0.055	33.263 ± 0.051
					Allende IV-2, unirradiated				
800	3.812	0.3720 ± 0.0069	0.3361 ± 0.0060	9.733 ± 0.027	104.47 ± 0.13	15.322 ± 0.040	79.715 ± 0.086	38.691 ± 0.054	32.767 ± 0.050
1000	0.4157	0.4596 ± 0.0254	0.4266 ± 0.0241	10.839 ± 0.073	126.38 ± 0.39	15.924 ± 0.088	81.820 ± 0.235	38.787 ± 0.112	32.705 ± 0.133
1100	0.3487	0.5566 ± 0.0216	0.4645 ± 0.0391	11.775 ± 0.128	123.63 ± 0.39	15.794 ± 0.129	82.857 ± 0.294	43.431 ± 0.193	40.355 ± 0.213
1200	1.157	0.5449 ± 0.0157	0.4665 ± 0.0156	8.755 ± 0.038	114.31 ± 0.21	16.014 ± 0.060	82.477 ± 0.190	41.619 ± 0.102	40.706 ± 0.096
1300	2.246	0.4776 ± 0.0094	0.4108 ± 0.0101	8.338 ± 0.031	111.47 ± 0.14	16.242 ± 0.033	82.045 ± 0.116	38.433 ± 0.075	32.466 ± 0.061
1350	3.260	0.4581 ± 0.0084	0.4119 ± 0.0089	8.299 ± 0.029	111.07 ± 0.12	16.169 ± 0.047	82.211 ± 0.120	38.053 ± 0.068	31.897 ± 0.062
1400	3.267	0.4720 ± 0.0069	0.4135 ± 0.0058	8.246 ± 0.027	122.04 ± 0.11	16.130 ± 0.033	82.249 ± 0.075	38.027 ± 0.054	31.873 ± 0.053
1450	1.680	0.4741 ± 0.0092	0.4103 ± 0.0096	8.256 ± 0.024	142.01 ± 0.22	16.171 ± 0.056	81.946 ± 0.143	38.307 ± 0.078	32.109 ± 0.082
1550	1.399	0.4764 ± 0.0092	0.4222 ± 0.0096	8.341 ± 0.033	168.70 ± 0.27	16.228 ± 0.045	82.092 ± 0.144	38.480 ± 0.080	32.461 ± 0.065
1700	0.8011	0.4822 ± 0.0189	0.4042 ± 0.0191	8.463 ± 0.040	178.68 ± 0.26	16.140 ± 0.062	81.972 ± 0.199	38.521 ± 0.092	32.723 ± 0.096
1800	0.08101	0.4065 ± 0.0474	0.3984 ± 0.0382	9.196 ± 0.165	170.08 ± 0.82	16.046 ± 0.169	82.187 ± 0.535	38.455 ± 0.429	32.357 ± 0.247
1900	0.04090	0.4359 ± 0.0704	0.3551 ± 0.0536	10.042 ± 0.177	159.99 ± 0.84	16.266 ± 0.264	81.870 ± 0.810	38.408 ± 0.479	33.529 ± 0.383
Total	18.51	0.4561 ± 0.0033	0.4013 ± 0.0033	8.755 ± 0.014	122.94 ± 0.18	15.978 ± 0.017	81.659 ± 0.044	38.770 ± 0.027	32.973 ± 0.029

				Allende 1-3					
800	0.2820	0.4201 ± 0.0338	0.3797 ± 0.0283	168.198 ± 0.639	109.50 ± 0.49	16.123 ± 0.166	284.244 ± 0.770	38.356 ± 0.257	33.202 ± 0.353
1000	1.166	0.5442 ± 0.0128	0.4479 ± 0.0105	60.449 ± 0.157	109.73 ± 0.26	16.034 ± 0.073	118.820 ± 0.279	44.387 ± 0.162	41.432 ± 0.192
1100	4.224	0.5047 ± 0.0074	0.4253 ± 0.0055	19.523 ± 0.047	107.63 ± 0.14	16.217 ± 0.052	85.815 ± 0.092	40.600 ± 0.086	35.835 ± 0.105
1150	7.257	0.4661 ± 0.0034	0.4103 ± 0.0058	15.891 ± 0.036	108.21 ± 0.09	16.251 ± 0.031	83.174 ± 0.098	38.208 ± 0.058	32.125 ± 0.060
1200	7.204	0.4726 ± 0.0052	0.4113 ± 0.0046	19.222 ± 0.040	111.65 ± 0.12	16.251 ± 0.029	83.274 ± 0.080	38.183 ± 0.065	32.216 ± 0.072
1250	3.431	0.4619 ± 0.0063	0.4185 ± 0.0053	35.376 ± 0.072	125.56 ± 0.19	16.265 ± 0.057	84.178 ± 0.152	38.292 ± 0.093	32.378 ± 0.094
1300	2.946	0.4574 ± 0.0075	0.4215 ± 0.0080	37.908 ± 0.073	128.48 ± 0.15	16.285 ± 0.061	84.059 ± 0.173	38.433 ± 0.114	32.276 ± 0.075
1350	1.369	0.4651 ± 0.0134	0.4185 ± 0.0124	60.895 ± 0.151	149.04 ± 0.21	16.383 ± 0.116	84.547 ± 0.223	38.468 ± 0.122	32.460 ± 0.106
1400	0.7625	0.4895 ± 0.0147	0.4319 ± 0.0135	93.086 ± 0.239	117.37 ± 0.41	16.218 ± 0.098	85.836 ± 0.252	38.929 ± 0.166	33.234 ± 0.167
1450	0.1904	0.4192 ± 0.0363	0.3690 ± 0.0414	98.372 ± 0.609	181.72 ± 0.82	16.408 ± 0.295	87.543 ± 0.557	38.866 ± 0.285	33.686 ± 0.420
1500	0.1256	0.4989 ± 0.0491	0.4600 ± 0.0376	98.539 ± 0.797	180.87 ± 0.98	16.705 ± 0.385	87.300 ± 0.776	38.014 ± 0.520	33.618 ± 0.449
1600	0.1270	0.4313 ± 0.0378	0.4815 ± 0.0295	103.443 ± 0.557	186.22 ± 0.95	16.642 ± 0.224	88.044 ± 1.117	39.680 ± 0.559	32.742 ± 0.448
1700	0.008733	0.2868 ± 0.2059	0.2210 ± 0.1493	100.185 ± 1.786	185.76 ± 2.77	17.271 ± 1.138	106.086 ± 3.000	39.150 ± 1.699	33.992 ± 1.381
Total	29.09	0.4748 ± 0.0024	0.4172 ± 0.0024	30.478 ± 0.026	118.04 ± 0.05	16.252 ± 0.017	87.377 ± 0.047	38.872 ± 0.031	33.180 ± 0.033
				Allende 1a-1					
800	0.04684	0.4413 ± 0.0803	0.4222 ± 0.0785	1471.368 ± 11.099	113.92 ± 1.19	15.425 ± 0.609	313.356 ± 3.458	37.533 ± 0.746	31.843 ± 0.704
1000	0.5085	0.5249 ± 0.0224	0.4591 ± 0.0245	465.179 ± 1.589	115.88 ± 0.36	16.341 ± 0.184	227.324 ± 0.553	43.009 ± 0.367	39.473 ± 0.376
1100	1.419	0.5619 ± 0.0135	0.4397 ± 0.0173	82.672 ± 0.183	114.61 ± 0.30	16.240 ± 0.092	98.522 ± 0.337	43.224 ± 0.196	40.083 ± 0.141
1150	4.165	0.4827 ± 0.0078	0.4234 ± 0.0091	35.597 ± 0.078	113.90 ± 0.15	16.250 ± 0.083	85.592 ± 0.181	38.735 ± 0.108	32.806 ± 0.100
1200	5.560	0.4662 ± 0.0084	0.4099 ± 0.0091	39.841 ± 0.058	121.47 ± 0.12	16.204 ± 0.057	86.383 ± 0.138	38.356 ± 0.108	32.339 ± 0.100
1250	2.885	0.4730 ± 0.0122	0.4111 ± 0.0110	48.123 ± 0.087	132.12 ± 0.27	16.458 ± 0.074	86.438 ± 0.153	38.357 ± 0.091	32.753 ± 0.136
1300	1.641	0.4595 ± 0.0077	0.4033 ± 0.0174	67.619 ± 0.210	149.44 ± 0.41	16.308 ± 0.102	87.851 ± 0.121	38.490 ± 0.149	32.802 ± 0.175
1350	0.6851	0.4746 ± 0.0248	0.4113 ± 0.0106	99.049 ± 0.357	178.78 ± 0.50	16.310 ± 0.150	90.702 ± 0.389	38.818 ± 0.236	33.644 ± 0.225
1400	0.2197	0.5055 ± 0.0370	0.4352 ± 0.0400	122.232 ± 0.787	199.93 ± 0.97	16.560 ± 0.245	93.152 ± 0.774	39.059 ± 0.455	33.528 ± 0.404
1450	0.09466	0.3889 ± 0.0522	0.4075 ± 0.0606	129.150 ± 1.385	206.73 ± 1.99	15.831 ± 0.358	96.341 ± 1.158	39.449 ± 0.591	34.328 ± 0.823
1500	0.03459	0.4224 ± 0.0780	0.4345 ± 0.1229	135.373 ± 2.089	207.60 ± 2.15	15.087 ± 0.581	103.056 ± 2.152	38.701 ± 1.168	32.859 ± 0.922
1600	0.08370	0.4924 ± 0.0466	0.4400 ± 0.0563	154.426 ± 1.267	222.17 ± 2.28	15.868 ± 0.476	101.737 ± 1.085	39.622 ± 0.784	35.143 ± 0.702
1700	0.02214	0.6216 ± 0.1579	0.3707 ± 0.1007	199.688 ± 3.794	261.00 ± 5.04	15.952 ± 0.693	122.156 ± 2.810	38.830 ± 1.125	35.018 ± 1.431
Total	17.36	0.4808 ± 0.0043	0.4171 ± 0.0047	67.451 ± 0.090	127.88 ± 0.09	16.275 ± 0.034	92.536 ± 0.080	39.032 ± 0.053	33.499 ± 0.053
				Allende 2a2					
800	0.1441	0.4752 ± 0.0391	0.4854 ± 0.0346	1333.226 ± 5.202	115.24 ± 0.74	15.912 ± 0.234	328.112 ± 1.806	38.945 ± 0.488	32.833 ± 0.443
1000	0.6155	0.5003 ± 0.0258	0.4569 ± 0.0180	463.287 ± 1.373	115.03 ± 0.40	16.109 ± 0.122	152.126 ± 0.728	42.040 ± 0.177	37.852 ± 0.238
1100	1.691	0.4985 ± 0.0103	0.4455 ± 0.0128	100.861 ± 0.155	111.14 ± 0.17	16.200 ± 0.076	94.807 ± 0.226	40.990 ± 0.155	36.847 ± 0.140
1150	1.829	0.4832 ± 0.0102	0.4309 ± 0.0119	58.917 ± 0.128	111.88 ± 0.18	16.225 ± 0.082	85.391 ± 0.221	38.361 ± 0.165	32.593 ± 0.134
1200	3.255	0.4725 ± 0.0083	0.4211 ± 0.0066	58.582 ± 0.083	113.11 ± 0.14	16.298 ± 0.060	84.623 ± 0.163	38.402 ± 0.098	32.082 ± 0.088
1250	2.169	0.4753 ± 0.0116	0.4193 ± 0.0093	62.639 ± 0.129	118.48 ± 0.16	16.139 ± 0.048	85.602 ± 0.121	37.996 ± 0.095	32.117 ± 0.130
1300	2.396	0.4764 ± 0.0068	0.4244 ± 0.0096	89.359 ± 0.182	141.07 ± 0.17	16.337 ± 0.079	87.359 ± 0.230	38.422 ± 0.158	32.575 ± 0.106
1350	2.443	0.4759 ± 0.0108	0.4171 ± 0.0066	79.009 ± 0.160	144.87 ± 0.17	16.268 ± 0.062	87.305 ± 0.174	38.434 ± 0.113	32.608 ± 0.124
1400	1.230	0.4521 ± 0.0143	0.4184 ± 0.0128	91.719 ± 0.192	157.72 ± 0.28	16.257 ± 0.091	89.129 ± 0.257	38.822 ± 0.138	32.800 ± 0.151
1450	0.3278	0.4729 ± 0.0261	0.3993 ± 0.0174	101.521 ± 0.561	170.48 ± 0.61	16.267 ± 0.167	91.753 ± 0.622	39.051 ± 0.191	33.982 ± 0.285
1500	0.1727	0.5439 ± 0.0327	0.5061 ± 0.0328	105.431 ± 0.701	176.11 ± 0.96	16.387 ± 0.299	92.728 ± 0.830	39.293 ± 0.443	33.718 ± 0.424
1600	0.1022	0.4983 ± 0.0405	0.4336 ± 0.0470	117.562 ± 0.903	183.66 ± 1.12	15.923 ± 0.246	95.610 ± 0.856	38.525 ± 0.580	32.931 ± 0.458
Total	16.38	0.4783 ± 0.0037	0.4266 ± 0.0034	101.710 ± 0.109	128.00 ± 0.07	16.244 ± 0.025	92.005 ± 0.078	38.815 ± 0.047	33.125 ± 0.044

Table 1. (Continued)

Temp (°C)	^{132}Xe × 10^{-10} cm^3 STP/g	^{132}Xe = 100							
		^{124}Xe	^{126}Xe	^{128}Xe	^{129}Xe	^{130}Xe	^{131}Xe	^{134}Xe	^{136}Xe
					Allende 4a1/b2				
800	0.2175	0.4506 ± 0.0548	0.4321 ± 0.0635	918.609 ± 6.970	109.77 ± 1.11	16.301 ± 0.338	178.233 ± 1.585	39.156 ± 0.577	31.928 ± 0.400
1000	1.112	0.4853 ± 0.0209	0.4274 ± 0.0212	402.801 ± 0.966	112.03 ± 0.49	15.685 ± 0.169	136.218 ± 0.588	40.498 ± 0.232	36.266 ± 0.201
1100	2.978	0.5021 ± 0.0140	0.4414 ± 0.0155	80.768 ± 0.213	108.59 ± 0.21	16.211 ± 0.091	87.681 ± 0.263	41.785 ± 0.152	38.368 ± 0.216
1200	15.23	0.4743 ± 0.0070	0.4185 ± 0.0064	31.963 ± 0.049	113.05 ± 0.11	16.305 ± 0.051	83.670 ± 0.121	38.208 ± 0.084	32.267 ± 0.072
1250	5.194	0.4637 ± 0.0049	0.4204 ± 0.0042	48.627 ± 0.055	130.78 ± 0.11	16.288 ± 0.030	84.835 ± 0.088	38.394 ± 0.039	32.453 ± 0.052
1300	4.469	0.4707 ± 0.0092	0.4089 ± 0.0102	44.851 ± 0.094	130.37 ± 0.22	16.289 ± 0.061	84.594 ± 0.180	38.252 ± 0.116	32.397 ± 0.098
1350	1.370	0.4713 ± 0.0078	0.4167 ± 0.0083	72.611 ± 0.109	154.38 ± 0.19	16.193 ± 0.063	86.723 ± 0.179	38.679 ± 0.081	32.789 ± 0.095
1400	0.9520	0.4736 ± 0.0144	0.4206 ± 0.0094	90.671 ± 0.181	172.18 ± 0.29	16.192 ± 0.075	87.937 ± 0.245	38.684 ± 0.136	33.050 ± 0.137
1450	0.1734	0.4950 ± 0.0444	0.4267 ± 0.0515	89.599 ± 0.615	173.48 ± 1.22	16.103 ± 0.396	90.810 ± 0.631	39.782 ± 0.586	31.905 ± 0.581
1500	0.1701	0.4543 ± 0.0694	0.3586 ± 0.0391	94.690 ± 0.665	178.16 ± 1.31	16.475 ± 0.459	93.746 ± 1.369	39.701 ± 0.655	33.685 ± 0.707
1550	0.004787	−0.2021 ± 0.6024	1.9340 ± 0.6641	72.023 ± 3.323	140.20 ± 4.46	14.251 ± 1.949	243.721 ± 10.423	31.457 ± 3.654	26.967 ± 3.241
1600	0.04671	0.5800 ± 0.1548	0.6016 ± 0.1344	100.649 ± 1.651	181.54 ± 3.27	16.782 ± 0.684	109.210 ± 3.352	37.787 ± 1.453	31.300 ± 0.961
1700	0.02788	0.7191 ± 0.2715	0.6877 ± 0.1526	106.980 ± 1.969	185.99 ± 3.39	15.686 ± 0.933	117.540 ± 3.634	42.072 ± 1.773	33.861 ± 1.322
Total	31.94	0.4750 ± 0.0040	0.4204 ± 0.0039	64.280 ± 0.089	122.26 ± 0.07	16.261 ± 0.029	87.276 ± 0.074	38.716 ± 0.048	33.072 ± 0.044
					Allende 12b1				
800	0.1312	0.4823 ± 0.0357	0.4296 ± 0.0401	337.165 ± 2.913	114.14 ± 1.03	15.907 ± 0.428	267.391 ± 1.608	37.841 ± 0.631	33.489 ± 0.655
1000	0.7105	0.5788 ± 0.0188	0.4893 ± 0.0179	99.262 ± 0.401	114.24 ± 0.44	16.082 ± 0.180	160.463 ± 0.645	44.264 ± 0.280	40.983 ± 0.238
1050	1.904	0.4558 ± 0.0115	0.4033 ± 0.0117	29.573 ± 0.103	117.90 ± 0.22	16.322 ± 0.086	85.677 ± 0.288	38.261 ± 0.174	32.380 ± 0.145
1100	1.605	0.5169 ± 0.0133	0.4275 ± 0.0106	42.848 ± 0.170	120.84 ± 0.30	16.061 ± 0.117	96.294 ± 0.278	40.825 ± 0.190	36.349 ± 0.198
1150	1.904	0.4558 ± 0.0115	0.4033 ± 0.0117	29.573 ± 0.103	117.90 ± 0.22	16.322 ± 0.086	85.677 ± 0.288	38.261 ± 0.174	32.380 ± 0.145
1200	2.700	0.4705 ± 0.0097	0.4078 ± 0.0087	31.690 ± 0.087	120.07 ± 0.15	16.222 ± 0.084	86.277 ± 0.155	38.258 ± 0.124	32.314 ± 0.084
1250	1.932	0.4676 ± 0.0132	0.4118 ± 0.0105	43.576 ± 0.141	131.03 ± 0.21	16.202 ± 0.108	87.745 ± 0.278	38.446 ± 0.119	32.402 ± 0.163
1300	2.547	0.4687 ± 0.0113	0.4331 ± 0.0110	56.515 ± 0.135	142.91 ± 0.26	16.285 ± 0.072	88.659 ± 0.123	38.417 ± 0.120	32.663 ± 0.126
1350	2.158	0.4644 ± 0.0121	0.4219 ± 0.0078	64.392 ± 0.181	151.29 ± 0.30	16.358 ± 0.098	88.697 ± 0.281	38.644 ± 0.130	32.626 ± 0.170
1400	0.8406	0.4532 ± 0.0226	0.4429 ± 0.0163	81.089 ± 0.291	165.84 ± 0.36	16.218 ± 0.137	90.552 ± 0.409	38.807 ± 0.163	32.972 ± 0.186
1450	0.2922	0.4631 ± 0.0292	0.4038 ± 0.0250	98.550 ± 0.493	179.55 ± 0.75	16.207 ± 0.284	93.067 ± 0.639	39.406 ± 0.351	33.735 ± 0.275
1500	0.1548	0.4418 ± 0.0428	0.4005 ± 0.0322	104.678 ± 0.840	184.43 ± 1.34	15.825 ± 0.311	96.239 ± 0.987	38.785 ± 0.411	32.875 ± 0.510
1600	0.04333	0.5491 ± 0.0747	0.5275 ± 0.0979	118.465 ± 1.653	195.85 ± 1.74	15.971 ± 0.645	103.668 ± 1.659	39.512 ± 1.118	34.066 ± 1.014
1700	0.009587	0.5343 ± 0.1916	0.3199 ± 0.1950	116.372 ± 2.361	188.81 ± 3.63	14.201 ± 0.882	133.105 ± 2.497	39.160 ± 1.700	31.084 ± 1.689
Total	16.93	0.4738 ± 0.0042	0.4202 ± 0.0036	51.276 ± 0.058	132.15 ± 0.09	16.240 ± 0.033	92.934 ± 0.088	38.901 ± 0.051	33.253 ± 0.050
					Allende 14b1				
800	0.09679	0.4327 ± 0.0428	0.3488 ± 0.0429	368.338 ± 2.605	113.91 ± 1.01	15.787 ± 0.400	307.403 ± 2.339	38.267 ± 0.728	33.006 ± 0.490
1000	0.9401	0.5168 ± 0.0184	0.4410 ± 0.0139	110.047 ± 0.282	113.11 ± 0.23	16.129 ± 0.128	154.977 ± 0.370	44.274 ± 0.171	42.459 ± 0.152
1100	2.672	0.5454 ± 0.0088	0.4471 ± 0.0080	35.133 ± 0.075	116.15 ± 0.16	16.153 ± 0.064	88.633 ± 0.143	43.297 ± 0.104	40.048 ± 0.078
1150	3.569	0.4733 ± 0.0053	0.4242 ± 0.0070	26.655 ± 0.058	115.11 ± 0.14	16.182 ± 0.054	84.270 ± 0.137	38.300 ± 0.086	32.558 ± 0.080
1200	3.564	0.4664 ± 0.0104	0.4150 ± 0.0053	29.676 ± 0.067	118.24 ± 0.15	16.222 ± 0.047	84.860 ± 0.165	38.271 ± 0.079	32.315 ± 0.088
1250	3.838	0.4638 ± 0.0085	0.4214 ± 0.0064	47.477 ± 0.079	134.49 ± 0.19	16.286 ± 0.048	86.197 ± 0.147	38.513 ± 0.072	32.507 ± 0.098
1300	1.780	0.4639 ± 0.0044	0.4126 ± 0.0041	53.536 ± 0.110	141.32 ± 0.26	16.183 ± 0.037	85.524 ± 0.076	38.412 ± 0.044	32.696 ± 0.128
1350	0.5053	0.4542 ± 0.0147	0.4104 ± 0.0238	106.406 ± 0.384	187.97 ± 0.47	16.409 ± 0.134	88.653 ± 0.458	38.580 ± 0.206	33.461 ± 0.233
1400	0.1841	0.4566 ± 0.0357	0.3742 ± 0.0306	167.633 ± 0.797	241.06 ± 1.26	16.399 ± 0.217	89.605 ± 0.643	39.017 ± 0.383	34.054 ± 0.448
1450	0.07992	0.4915 ± 0.0411	0.4650 ± 0.0489	176.248 ± 1.259	250.11 ± 2.53	16.484 ± 0.511	92.764 ± 1.092	41.155 ± 0.529	34.334 ± 0.510
1500	0.04718	0.4724 ± 0.0716	0.3789 ± 0.0724	169.699 ± 1.718	245.97 ± 1.92	15.849 ± 0.326	94.302 ± 1.213	38.563 ± 0.671	34.391 ± 0.489
1600	0.01944	0.5220 ± 0.0972	0.2867 ± 0.0898	179.435 ± 2.014	250.42 ± 1.65	15.827 ± 0.829	106.920 ± 1.897	42.142 ± 1.047	35.083 ± 0.738
1700	0.001381	0.7455 ± 0.4933	−0.3753 ± 0.2747	81.507 ± 2.891	153.87 ± 8.07	12.919 ± 2.152	197.817 ± 9.201	38.952 ± 3.682	29.762 ± 2.330
Total	17.30	0.4815 ± 0.0036	0.4234 ± 0.0029	47.505 ± 0.044	127.40 ± 0.07	16.213 ± 0.023	91.000 ± 0.067	39.484 ± 0.036	34.267 ± 0.039

				Allende 25s1-tw1					
800	0.2708	0.4702 ± 0.0396	0.4372 ± 0.0324	128.397 ± 0.614	109.09 ± 0.47	15.920 ± 0.231	259.403 ± 1.432	37.950 ± 0.267	32.640 ± 0.358
1000	0.3013	0.5343 ± 0.0300	0.4333 ± 0.0315	66.033 ± 0.406	110.95 ± 0.59	15.918 ± 0.219	146.374 ± 0.923	42.904 ± 0.311	38.822 ± 0.395
1100	0.3606	0.5217 ± 0.0254	0.4181 ± 0.0262	48.737 ± 0.229	111.18 ± 0.39	16.181 ± 0.200	129.571 ± 0.655	42.803 ± 0.274	39.207 ± 0.312
1150	6.476	0.4851 ± 0.0054	0.4273 ± 0.0053	21.853 ± 0.047	111.17 ± 0.11	16.187 ± 0.052	90.226 ± 0.081	39.173 ± 0.084	33.741 ± 0.070
1200	4.299	0.4554 ± 0.0087	0.4070 ± 0.0058	26.830 ± 0.055	118.04 ± 0.13	16.274 ± 0.066	87.190 ± 0.138	38.269 ± 0.079	32.237 ± 0.085
1250	2.875	0.4565 ± 0.0099	0.4202 ± 0.0080	46.569 ± 0.102	135.51 ± 0.28	16.248 ± 0.074	89.699 ± 0.248	38.482 ± 0.101	32.552 ± 0.093
1300	2.123	0.4721 ± 0.0083	0.3896 ± 0.0090	50.316 ± 0.076	138.17 ± 0.25	16.198 ± 0.070	89.090 ± 0.218	38.432 ± 0.095	32.342 ± 0.162
1350	0.8577	0.4666 ± 0.0143	0.4226 ± 0.0152	72.789 ± 0.277	158.68 ± 0.27	16.274 ± 0.122	91.279 ± 0.420	38.751 ± 0.232	32.764 ± 0.166
1400	0.5978	0.4237 ± 0.0203	0.3793 ± 0.0190	92.132 ± 0.242	176.14 ± 0.47	16.047 ± 0.186	91.141 ± 0.316	38.648 ± 0.293	33.273 ± 0.177
1450	0.1945	0.4684 ± 0.0354	0.3776 ± 0.0374	114.719 ± 0.736	195.28 ± 0.91	16.315 ± 0.255	94.033 ± 0.812	38.613 ± 0.443	34.494 ± 0.413
1500	0.07985	0.5326 ± 0.0653	0.4478 ± 0.0475	127.779 ± 0.990	206.37 ± 1.38	16.359 ± 0.278	99.232 ± 1.045	40.462 ± 0.670	33.876 ± 0.768
1600	0.05646	0.6198 ± 0.0715	0.4449 ± 0.0530	131.257 ± 1.540	206.90 ± 1.75	15.699 ± 0.536	101.504 ± 1.668	38.829 ± 0.765	33.463 ± 0.706
1700	0.02727	0.5674 ± 0.0886	0.4172 ± 0.0972	184.321 ± 2.069	253.49 ± 2.77	16.558 ± 0.773	119.806 ± 2.294	40.088 ± 0.967	36.227 ± 1.332
Total	18.52	0.4713 ± 0.0036	0.4151 ± 0.0031	39.541 ± 0.039	125.70 ± 0.08	16.210 ± 0.030	93.698 ± 0.074	38.848 ± 0.043	33.171 ± 0.042
				Vigarano 2226					
1100	17.02	0.4639 ± 0.0056	0.4214 ± 0.0068	35.970 ± 0.054	106.47 ± 0.14	16.315 ± 0.072	82.797 ± 0.131	38.315 ± 0.086	32.469 ± 0.072
1200	60.39	0.4652 ± 0.0041	0.4127 ± 0.0023	19.598 ± 0.030	106.71 ± 0.08	16.191 ± 0.028	82.212 ± 0.079	38.011 ± 0.045	31.825 ± 0.043
1250	16.34	0.4551 ± 0.0069	0.3990 ± 0.0075	20.540 ± 0.040	108.62 ± 0.17	16.165 ± 0.058	82.574 ± 0.142	38.102 ± 0.088	32.142 ± 0.075
1300	11.43	0.4596 ± 0.0078	0.4044 ± 0.0077	22.341 ± 0.081	108.52 ± 0.16	16.250 ± 0.063	82.157 ± 0.151	38.041 ± 0.164	32.027 ± 0.104
1350	3.025	0.4559 ± 0.0189	0.3932 ± 0.0190	29.281 ± 0.105	112.00 ± 0.27	16.115 ± 0.146	82.496 ± 0.262	38.033 ± 0.181	32.332 ± 0.173
1400	0.3968	0.5077 ± 0.0391	0.3937 ± 0.0413	56.842 ± 0.379	128.61 ± 0.73	15.875 ± 0.345	82.803 ± 0.740	38.124 ± 0.391	33.765 ± 0.465
1450	0.07638	0.4162 ± 0.0941	0.2464 ± 0.0923	66.293 ± 1.203	134.51 ± 2.47	15.217 ± 0.636	82.800 ± 2.160	39.806 ± 1.294	33.150 ± 1.690
1500	0.04309	0.4085 ± 0.1432	0.2625 ± 0.9310	59.143 ± 1.641	131.25 ± 2.96	16.422 ± 0.952	87.923 ± 2.714	39.489 ± 1.688	34.141 ± 1.289
1550	0.02411	0.4523 ± 0.1542	0.4885 ± 0.2350	53.041 ± 2.691	127.49 ± 3.34	17.220 ± 1.339	81.855 ± 2.910	39.332 ± 2.366	37.823 ± 1.656
1600	0.01483	−0.1607 ± 0.2840	0.4777 ± 0.2862	46.334 ± 1.946	120.58 ± 3.14	16.855 ± 1.956	77.969 ± 4.193	42.391 ± 2.555	29.821 ± 2.081
1800	0.1344	0.3724 ± 0.0660	0.2643 ± 0.0519	17.346 ± 0.445	106.92 ± 1.31	15.578 ± 0.506	81.336 ± 1.226	39.057 ± 0.710	32.814 ± 0.924
Total	108.9	0.4625 ± 0.0028	0.4102 ± 0.0022	23.032 ± 0.025	107.41 ± 0.06	16.208 ± 0.022	82.362 ± 0.056	38.080 ± 0.036	32.020 ± 0.031
				Efremovka E-80					
800	0.7398	0.3924 ± 0.0123	0.3219 ± 0.0185	13.007 ± 0.097	97.94 ± 0.36	15.328 ± 0.215	79.706 ± 0.461	38.790 ± 0.234	32.976 ± 0.263
900	0.6721	0.3764 ± 0.0231	0.3545 ± 0.0185	57.092 ± 0.348	102.02 ± 0.45	15.426 ± 0.200	83.512 ± 0.390	38.587 ± 0.306	32.273 ± 0.258
1000	2.644	0.4441 ± 0.0108	0.3877 ± 0.0098	188.172 ± 0.227	176.43 ± 0.27	16.349 ± 0.078	87.276 ± 0.196	38.060 ± 0.098	32.220 ± 0.122
1050	1.876	0.4778 ± 0.0152	0.4050 ± 0.0141	175.030 ± 0.359	214.92 ± 0.49	16.322 ± 0.108	87.824 ± 0.285	38.420 ± 0.192	32.303 ± 0.154
1100	0.8237	0.4617 ± 0.0205	0.4255 ± 0.0154	155.633 ± 0.432	212.53 ± 0.52	16.107 ± 0.163	88.868 ± 0.420	38.666 ± 0.271	33.234 ± 0.220
1150	1.116	0.4905 ± 0.0161	0.4398 ± 0.0124	130.589 ± 0.514	191.25 ± 0.46	16.211 ± 0.115	89.450 ± 0.358	40.072 ± 0.237	35.242 ± 0.212
1200	1.923	0.5255 ± 0.0110	0.4395 ± 0.0120	79.210 ± 0.154	145.48 ± 0.24	16.115 ± 0.078	85.548 ± 0.302	42.001 ± 0.189	37.995 ± 0.194
1250	0.9746	0.5036 ± 0.0235	0.3880 ± 0.0148	66.425 ± 0.275	159.10 ± 0.43	16.461 ± 0.099	84.168 ± 0.388	41.086 ± 0.263	36.602 ± 0.287
1300	3.233	0.4794 ± 0.0074	0.4102 ± 0.0093	143.549 ± 0.146	315.49 ± 0.31	16.199 ± 0.082	87.584 ± 0.203	40.319 ± 0.095	34.666 ± 0.124
1350	2.650	0.4496 ± 0.0128	0.4106 ± 0.0114	150.860 ± 0.234	240.16 ± 0.31	16.266 ± 0.079	85.355 ± 0.172	38.756 ± 0.166	33.127 ± 0.125
1400	2.031	0.4802 ± 0.0138	0.4291 ± 0.0112	199.803 ± 0.423	273.38 ± 0.61	16.222 ± 0.116	84.816 ± 0.220	38.512 ± 0.134	33.052 ± 0.145
1450	0.6975	0.4773 ± 0.0207	0.4163 ± 0.0212	259.425 ± 0.936	333.28 ± 1.00	16.423 ± 0.108	85.562 ± 0.508	38.651 ± 0.236	32.803 ± 0.217
1500	0.03584	0.3897 ± 0.1117	0.4857 ± 0.0733	422.987 ± 3.671	467.64 ± 3.72	16.961 ± 0.716	89.331 ± 2.152	39.280 ± 1.197	33.258 ± 1.200
1550	0.01050	0.7904 ± 0.2622	0.5827 ± 0.2221	497.556 ± 8.898	521.99 ± 9.11	14.981 ± 1.308	103.679 ± 4.184	42.416 ± 2.148	35.647 ± 1.740
1600	0.004794	−0.2948 ± 0.3034	0.4161 ± 0.3123	498.592 ± 10.012	509.37 ± 11.27	17.486 ± 1.942	104.263 ± 4.967	43.540 ± 3.351	33.842 ± 2.356
1700	0.009753	0.0544 ± 0.3188	0.3439 ± 0.1827	474.415 ± 8.996	505.40 ± 10.90	17.189 ± 1.040	97.406 ± 4.764	36.865 ± 1.750	32.023 ± 2.088
1900	0.03435	0.3255 ± 0.0911	0.3507 ± 0.0889	126.147 ± 2.271	205.49 ± 2.97	16.479 ± 0.615	82.383 ± 1.454	40.775 ± 1.125	32.254 ± 0.949
Total	19.48	0.4685 ± 0.0041	0.4078 ± 0.0038	146.192 ± 0.099	221.54 ± 0.13	16.195 ± 0.031	86.262 ± 0.081	39.371 ± 0.051	33.905 ± 0.050

Table 1. (Continued)

Temp (°C)	^{132}Xe × 10^{-10} cm^3 STP/g	^{132}Xe = 100							
		^{124}Xe	^{126}Xe	^{128}Xe	^{129}Xe	^{130}Xe	^{131}Xe	^{134}Xe	^{136}Xe
				Leoville LV1					
800	1.119	0.3576 ± 0.0191	0.3618 ± 0.0142	20.839 ± 0.128	98.14 ± 0.33	15.173 ± 0.146	146.133 ± 0.475	39.027 ± 0.235	33.107 ± 0.172
1000	1.010	0.3775 ± 0.0191	0.3742 ± 0.0135	202.665 ± 0.527	105.83 ± 0.33	15.357 ± 0.157	687.431 ± 1.766	38.860 ± 0.165	33.207 ± 0.246
1050	0.2782	0.4689 ± 0.0324	0.3713 ± 0.0314	230.913 ± 1.085	113.68 ± 0.67	15.314 ± 0.174	1490.870 ± 6.736	40.168 ± 0.424	34.612 ± 0.442
1100	0.2462	0.4945 ± 0.0489	0.3721 ± 0.0287	142.385 ± 0.791	115.34 ± 0.81	15.482 ± 0.206	1446.491 ± 8.240	40.417 ± 0.367	35.138 ± 0.436
1150	0.3855	0.4401 ± 0.0301	0.3526 ± 0.0248	121.472 ± 0.643	123.08 ± 0.70	15.450 ± 0.213	665.920 ± 3.549	42.362 ± 0.423	38.204 ± 0.307
1200	0.3814	0.5250 ± 0.0317	0.4242 ± 0.0302	129.129 ± 0.628	137.45 ± 0.54	16.180 ± 0.216	300.204 ± 1.407	47.184 ± 0.476	45.456 ± 0.525
1250	0.4936	0.6284 ± 0.0316	0.4628 ± 0.0288	113.121 ± 0.401	143.22 ± 0.52	16.012 ± 0.203	160.360 ± 0.808	49.256 ± 0.434	48.547 ± 0.423
1300	0.4052	0.4730 ± 0.0306	0.4524 ± 0.0344	164.552 ± 0.621	174.61 ± 0.75	16.110 ± 0.181	253.578 ± 1.261	43.848 ± 0.536	41.308 ± 0.381
1350	1.344	0.5039 ± 0.0158	0.4232 ± 0.0186	169.471 ± 0.348	187.30 ± 0.41	15.827 ± 0.083	194.318 ± 0.559	42.979 ± 0.187	38.873 ± 0.174
1400	2.571	0.4888 ± 0.0118	0.4177 ± 0.0122	198.987 ± 0.311	225.69 ± 0.29	16.104 ± 0.080	142.955 ± 0.345	41.715 ± 0.140	37.846 ± 0.122
1450	1.854	0.4796 ± 0.0143	0.4122 ± 0.0122	197.322 ± 0.365	241.32 ± 0.44	15.901 ± 0.091	121.598 ± 0.359	39.849 ± 0.176	35.297 ± 0.201
1500	0.8241	0.4720 ± 0.0146	0.3818 ± 0.0171	192.074 ± 0.590	239.95 ± 0.65	16.179 ± 0.149	118.383 ± 0.400	39.494 ± 0.295	34.781 ± 0.300
1550	0.3590	0.4443 ± 0.0283	0.3979 ± 0.0403	247.940 ± 1.078	283.41 ± 0.93	16.111 ± 0.225	130.054 ± 0.908	38.726 ± 0.468	34.722 ± 0.310
1600	0.05246	0.3200 ± 0.0654	0.3648 ± 0.0754	378.359 ± 3.402	373.71 ± 3.93	16.027 ± 0.464	185.159 ± 3.058	40.453 ± 0.595	36.896 ± 0.742
1700	0.02177	0.6197 ± 0.1397	0.6804 ± 0.1080	508.295 ± 7.741	472.39 ± 7.91	15.232 ± 0.799	234.632 ± 5.549	42.044 ± 1.864	38.705 ± 1.535
1900	0.06460	0.4178 ± 0.0811	0.3452 ± 0.0738	395.300 ± 3.091	378.59 ± 4.07	14.821 ± 0.501	220.656 ± 2.549	41.123 ± 1.310	35.803 ± 0.630
Total	11.41	0.4675 ± 0.0056	0.4038 ± 0.0054	171.332 ± 0.145	188.55 ± 0.15	15.921 ± 0.038	281.258 ± 0.428	41.322 ± 0.072	37.059 ± 0.069
				Leoville LV2					
800	3.775	0.3687 ± 0.0093	0.3316 ± 0.0080	11.575 ± 0.069	98.43 ± 0.15	15.152 ± 0.084	82.792 ± 0.231	38.989 ± 0.116	33.251 ± 0.119
1000	1.579	0.3637 ± 0.0111	0.3405 ± 0.0097	120.624 ± 0.256	103.20 ± 0.24	15.574 ± 0.073	142.982 ± 0.425	39.444 ± 0.212	33.674 ± 0.152
1050	0.6549	0.4714 ± 0.0256	0.3738 ± 0.0156	96.529 ± 0.433	110.03 ± 0.62	15.770 ± 0.210	146.448 ± 0.807	40.821 ± 0.330	37.451 ± 0.348
1100	1.399	0.4958 ± 0.0193	0.4492 ± 0.0133	68.508 ± 0.243	113.85 ± 0.30	15.924 ± 0.103	103.080 ± 0.350	41.873 ± 0.265	38.844 ± 0.180
1150	4.078	0.4846 ± 0.0105	0.4241 ± 0.0087	34.051 ± 0.083	111.79 ± 0.18	16.058 ± 0.079	85.699 ± 0.179	40.840 ± 0.111	36.199 ± 0.110
1200	5.849	0.4731 ± 0.0066	0.4238 ± 0.0077	19.665 ± 0.067	108.58 ± 0.14	16.220 ± 0.053	83.189 ± 0.162	39.410 ± 0.079	34.194 ± 0.084
1250	5.136	0.4558 ± 0.0078	0.4102 ± 0.0077	16.873 ± 0.054	107.40 ± 0.17	16.120 ± 0.057	82.606 ± 0.200	38.280 ± 0.113	32.627 ± 0.101
1300	7.150	0.4695 ± 0.0066	0.4138 ± 0.0066	23.058 ± 0.049	110.97 ± 0.12	16.129 ± 0.057	83.442 ± 0.133	38.453 ± 0.086	32.542 ± 0.088
1350	21.62	0.4543 ± 0.0024	0.4047 ± 0.0031	20.014 ± 0.020	109.89 ± 0.09	16.212 ± 0.033	82.630 ± 0.083	38.163 ± 0.061	32.254 ± 0.038
1400	13.52	0.4530 ± 0.0047	0.4029 ± 0.0052	16.329 ± 0.027	107.48 ± 0.11	16.161 ± 0.030	82.425 ± 0.088	38.193 ± 0.056	32.232 ± 0.053
1450	0.5709	0.4193 ± 0.0241	0.4178 ± 0.0249	22.902 ± 0.171	109.70 ± 0.49	16.256 ± 0.192	83.308 ± 0.519	38.445 ± 0.259	32.439 ± 0.261
1500	0.2381	0.5023 ± 0.0439	0.4248 ± 0.0431	31.210 ± 0.333	110.26 ± 0.85	16.339 ± 0.249	82.418 ± 0.803	38.117 ± 0.434	33.730 ± 0.491
1550	0.05322	0.3386 ± 0.0545	0.1897 ± 0.0641	43.153 ± 0.915	113.55 ± 1.18	15.260 ± 0.759	87.036 ± 2.324	40.492 ± 0.771	37.430 ± 0.763
1600	0.03325	0.5730 ± 0.0920	0.2009 ± 0.0990	49.224 ± 0.741	108.48 ± 2.19	16.438 ± 0.797	87.038 ± 2.212	48.535 ± 1.328	45.927 ± 1.419
1700	0.02853	0.5746 ± 0.1249	0.3726 ± 0.1102	75.646 ± 1.872	101.14 ± 1.69	13.816 ± 0.640	86.305 ± 2.604	61.748 ± 2.123	68.732 ± 1.621
1900	0.01624	0.6637 ± 0.1628	0.7882 ± 0.1549	24.437 ± 0.986	100.76 ± 3.59	15.856 ± 1.238	90.537 ± 3.917	38.745 ± 1.838	33.381 ± 2.018
Total	65.70	0.4533 ± 0.0020	0.4035 ± 0.0021	24.035 ± 0.019	108.58 ± 0.05	16.086 ± 0.017	85.461 ± 0.048	38.691 ± 0.030	33.046 ± 0.025

Table 2. Apparent trapped Xe compositions and I-Xe ages (relative to Shallowater) for dark inclusions from Allende, Vigarano, Efremovka and Leoville.

Sample	Weight (mg)	$^{129*}Xe \times 10^{-10}$ cm^3STP/g (corr.%)	I-Xe age (Ma)	# points on isochron	Apparent[b] trapped Xe	
					$^{129}Xe/^{132}Xe$	$^{128}Xe/^{132}Xe$
			Allende			
4294-1[a]	42.33	10.43 (79%)	−1.9 ± 0.4	5	0.86	0.20
4301-1	18.37	4.29 (89%)	−1.8 ± 0.1	9	0.92	0.21
4314-3	18.70	3.17 (65%)	−1.2 ± 0.1	8	0.95	0.18
4320-1	13.98	4.14 (71%)	−0.9 ± 0.2	9	1.00	0.12
4884-1	35.38	3.95 (94%)	−1.0 ± 0.1	11	1.03	0.10
4884-2	18.79	5.93 (92%)	−1.7 ± 0.3	9	0.83	0.32
4884-3	28.69	5.90 (84%)	−0.4 ± 0.1	8	1.04 (OC)	0.083 (OC)
4884-5	18.79	5.53 (91%)	−0.8 ± 0.1	9	1.03	0.096
4884-6	26.78	5.48 (92%)	−0.9 ± 0.1	10	1.03	0.093
IV-1	29.21	3.28 (91%)	−1.6 ± 0.2	3 (LT)	0.96	0.17
			−1.3 ± 0.1	6 (HT)	0.99	0.14
IV-2	20.14	3.20 (83%)	−1.1 ± 0.2	6	1.01	0.11
1-3	41.14	4.09 (94%)	−1.4 ± 0.1	9	1.02	0.11
1a-1	28.49	4.15 (85%)	−1.6 ± 0.2	8	0.96	0.17
2a-2	39.01	3.93 (53%)	−5.7 ± 0.4	5	0.69	0.41
4a1/b2	16.46	5.84 (48%)	−1.8 ± 0.2	8	0.97	0.16
12b1	29.64	4.77 (87%)	−2.1 ± 0.2	10	0.99	0.14
14b1	45.29	4.05 (80%)	−1.9 ± 0.1	10	0.99	0.14
25s1-tw1	34.99	4.02 (87%)	−1.1 ± 0.1	9	1.02	0.11
			Vigarano			
2226	10.99	3.73 (89%)	8.6 ± 0.6	10	1.0	0.14
			Efremovka			
E80[a]	27.49	22.90 (83%)	−0.9 ± 0.3	3 (LT)	0.83	0.31
			−1.0 ± 0.5	7 (HT)	1.04 (OC)	0.083 (OC)
			Leoville			
LV1	24.71	9.65 (48%)	3.0 ± 0.1	6	1.03	0.10
LV2	23.58	3.02 (69%)	9.9 ± 1.0	5	1.03	0.10

[a] Corrections for fission Xe resulted in larger uncertainties so alternate normalization (^{130}Xe not ^{132}Xe) was used for the isochron, apparent trapped components, and I-Xe age calculations.
[b] The apparent trapped $^{129}Xe/^{132}Xe$ was computed by fixing $^{128}Xe/^{132}Xe$ ratio on the isochron to the OC value; the apparent trapped $^{128}Xe/^{132}Xe$ was computed by fixing $^{129}Xe/^{132}Xe$ ratio on the isochron to the OC value.

tributions at these isotopes, with the precision of the data normally favoring the more abundant ^{132}Xe. The relatively short cosmic ray exposure age of Allende, and carbonaceous chondrites in general, is reflected in the virtual absence of cosmogenic Xe in the DIs, eliminating the need for cosmogenic corrections of ^{130}Xe if that isotope were chosen for normalization. However, the more abundant ^{132}Xe is the preferred normalization, and corrections were made for minor amounts of ^{132}Xe produced by neutron fission of ^{235}U in the reactor. Fission corrections were made by partitioning the measured $^{134}Xe/^{132}Xe$ ratio between that of ^{235}U fission and nominal trapped Xe (due to neutron capture on ^{135}Xe, the $^{136}Xe/^{132}Xe$ ratio cannot be used unless the actual fission spectrum for this particular irradiation is carefully monitored). This typically changes the resulting I-Xe ages by less than a few hundred thousand years and generally improves the χ-squared fit to the isochron. Correcting ^{132}Xe for fission contributions moves the data points directly away from the origin, approximately along the isochron, so the uncertainty introduced to the isochron is much less than the uncertainty of the correction procedure. The maximum fission contribution to ^{132}Xe (10.4%) was observed in the 1450°C fraction of 4884-2 (2.0% contribution for the whole sample, and for all other samples it was much less than 1%). Although both ^{130}Xe and ^{132}Xe normalizations give the same ages, a useful check, we usually prefer ^{132}Xe normalization because of the smaller uncertainties it yields.

At the lower temperatures (extracted from the less retentive sites), some $^{129*}Xe$ may have been lost and/or terrestrial iodine contamination may have occurred resulting in $^{128*}Xe$ unaccompanied by a full complement of radiogenic $^{129*}Xe$. These fractions are obvious in both the thermal release patterns and in departures from the isochron in 3-isotope plots. However, above a certain temperature the two iodine-derived contributions are released in fixed proportion, defining linear arrays with many consecutive extractions. In these particular samples, the isochrons contain most of the iodine-derived Xe (generally more than 80%, column 3 of Table 2). Only those temperature fractions defining the isochrons are shown in the figures, and these are indicated in boldface in Table 1.

Figure 2 shows Allende DI IV-1 which has nine approximately collinear points, all with tiny error bars. However, when viewed in two groups, the six higher temperature fractions define the major isochron, a mixing line that seems to be even more co-linear than the small errors would suggest. It has a χ-squared fit of 0.2 (χ-squared less than unity is attributed to overstating the errors) and an I-Xe age that is 1.3 ± 0.1 Ma older than Shallowater. What is surprising here is that the isochron does not pass through the normal planetary composi-

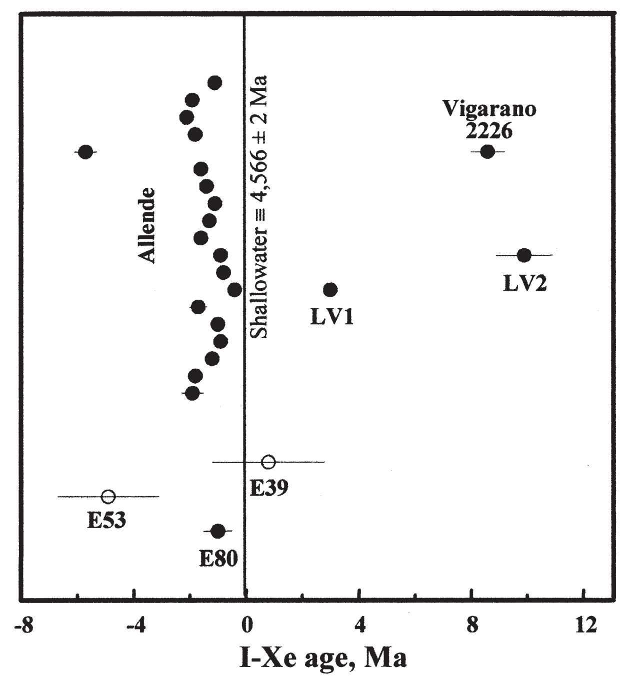

Fig. 1. I-Xe ages of 18 different Allende dark inclusions, Vigarano 2226, Leoville LV1 and LV2, Efremovka E80 (this work), and Efremovka E53 and E39 dark inclusions from a previous study (Swindle et al., 1998; Krot et al., 1999). Negative numbers indicate samples older than the Shallowater reference, which has an absolute I-Xe age of 4.566 ± 0.002 Ga (Nichols et al., 1994).

tion (shown here as OC), but rather is "subplanetary" having a lower than planetary value for the ^{129}Xe/^{132}Xe ratio (if the ^{128}Xe/^{132}Xe trapped ratio were planetary). As discussed above, such a trapped composition could not be related to planetary Xe by open system decay of ^{129}I, and corresponds to no known component. A second, lower temperature, isochron can be obtained from the three temperature fractions (1350, 1400, and 1450°C), each also with tiny error bars and highly co-linear. The thermal release profiles suggest that the lower temperature isochron probably corresponds to a different iodine host phase. This second isochron, identical within error in age to the main isochron (same slope and same initial iodine), requires a different trapped Xe composition. The release pattern of the radiogenic xenon (Fig. 2) shows that most of the ^{129*}Xe (~91%) is included in the nine temperature fractions defining these two isochrons.

Figure 3 is the isochron plot of Allende DI 4884-5, whose nine temperature fractions yield a straight line with χ-squared fit of 0.5. This sample has an I-Xe age of 0.8 ± 0.1 Ma before Shallowater (older), and it too requires a "subplanetary" trapped component, but one different from that of DI IV-1.

Figure 4 shows DI 4884-2, with nine consecutive temperature fractions defining the isochron, an I-Xe age of 1.7 ± 0.3 Ma before Shallowater, and the most "subplanetary" trapped composition of all the DIs studied here. In fact, 20 of the 22 DIs require "subplanetary" trapped Xe of diverse compositions. Although trapped Xe must lie somewhere on each of these isochrons, we cannot distinguish exactly where on these mixing lines it is located. Either the ^{129}Xe/^{132}Xe ratio is really "subplanetary" (lower than Q-Xe) or the ^{128}Xe/^{132}Xe ratio is anomalously high (higher than Q-Xe), or some combination of the two.

This point is clarified by a comparison between two samples of DI IV-2, one of which was irradiated and the other unirradiated (Fig. 5). As for most of the other DIs, "subplanetary" Xe is required for the irradiated sample because its isochron passes below normal planetary composition (OC or Q-Xe). In the unirradiated sample, no ^{128*}Xe is produced by neutron capture from ^{127}I, so the stepwise heating data from the unirradiated sample should define a vertical mixing line between trapped Xe and the iodine-derived component, now at infinity in the +y-direction. Such is the case, as can be seen in Figure 5. The true trapped Xe composition should, therefore, lie at the intersection of the two mixing lines, one for the irradiated sample and one for the unirradiated sample. The unirradiated sample of DI IV-2 shows that the ^{128}Xe/^{132}Xe in trapped Xe is perfectly normal because its vertical line passes right through OC, with the intersection below, suggesting that it is really the ^{129}Xe/^{132}Xe ratio in the apparent trapped component that is anomalously low. However, we have argued that it is impossible to evolve such a component in the solar system because ^{129}I decay cannot appreciably change trapped Xe in an open system and, if decay occurred in a closed system, ^{129}Xe in the apparent trapped

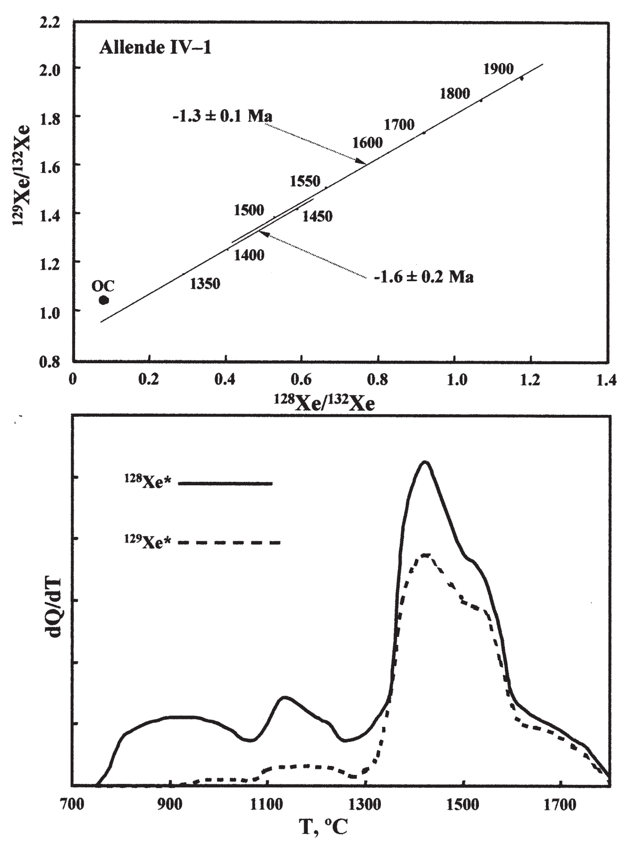

Fig. 2. Three-isotope plot and release profiles for Allende dark inclusion IV-I. Minor fission corrections (typically <1%) were made to ^{132}Xe. Only the points that define the isochrons are shown (indicated in bold in Table 1). Release profiles are shown for ^{128*}Xe and ^{129*}Xe after subtraction of the trapped (OC-Xe) component. dQ/dT is the fraction of radiogenic xenon (cm^3 STP) released per fixed temperature extraction step. The I-Xe system shows a double structure, reflected in the release profiles as well as the isochrons.

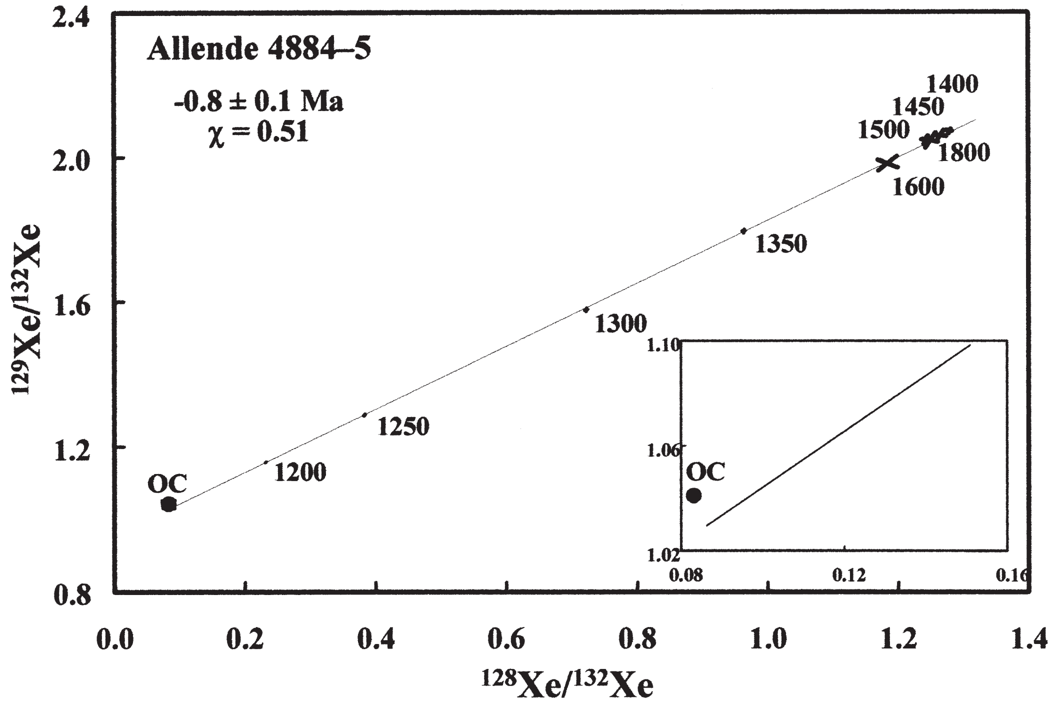

Fig. 3. I-Xe plot for Allende DI 4884-5, with nine consecutive temperature fractions defining the isochron. Although the χ-squared fit to a straight line of 0.51 suggests a somewhat over-estimate of the errors, it indicates that the isochron conforms well to two-component mixing between iodine-derived and "subplanetary" trapped Xe.

component would be too high, not too low. Moreover, there are other problems.

Allende DI 4320-1, with nine temperature fractions, provides an I-Xe age of -0.9 ± 0.2, not significantly different from the age of DI 4884-3 (-0.4 ± 0.1), but 4320-1 requires a "subplanetary" trapped component, whereas DI 4884-3 requires trapped Xe of normal planetary composition. Moreover, DI IV-1 has two isochrons of the same age but different trapped components, as does Efremovka E80. That is, different trapped components are required, not only for samples of the same age, but for different minerals within the same samples.

Perhaps these apparent trapped Xe components are actually mixtures of normal trapped Xe and other Xe components, with the variations reflecting different mixing ratios. Combinations of Q-Xe and various known components were investigated (Xe-N and Xe-G [Ott, 2002], U-Xe [Pepin et al., 1995]) but none of the mixtures could produce any of the observed end-member compositions.

Figure 6 shows the isochron for Allende CAI-3803 (Pravdivtseva et al., 2003c). It consists of only three points, but these are very co-linear and correspond to the peak ^{129*}Xe release (85% of the ^{129*}Xe). This isochron would require a *negative* value for the ^{129}Xe/^{130}Xe ratio in the trapped component (for a ^{128}Xe/^{130}Xe ratio of normal planetary composition, as required by the unirradiated sample of Allende DI IV-2). This contradiction leads us to conclude: 1) That the ^{129}Xe/^{130}Xe ratio, inferred for the trapped component by extrapolating to a planetary value of the ratio ^{128}Xe/^{130}Xe, cannot be correct; 2) That it is not the ^{129}Xe/^{130}Xe ratio in trapped Xe that is anomalous, but the ^{128}Xe/^{130}Xe ratio; and 3) Comparison of the two Allende DI IV-2 samples convincingly demonstrates that the neutron irradiation itself adds ^{128*}Xe to the trapped component. This observation leads to the inescapable conclusion that the trapped component in these samples is really an intimate mixture of Xe and iodine, some of which is converted to ^{128*}Xe by irradiation. The fact that we have never observed Xe in any extraction from any sample with a ^{129}Xe/^{132}Xe ratio that is lower than planetary is consistent with this explanation.

That a uniform but unusual trapped Xe component can be produced in the reactor from an iodine-Xe mixture may provide clues about the location of this component. Fractionation of parent from daughter forms the basis of radionuclear dating. However, for the trapped component, we are proposing that the iodine-produced ^{128}Xe and the original planetary Xe do not fractionate by thermal processes. They appear to be inseparable in stepwise heating. Chemical fractionation clearly occurs during mineral formation, such as precipitation of sodalite in which iodine is a structural member, providing the framework for I-Xe dating. However, fractionation may not occur when Xe and iodine are both trapped on surfaces or grain boundaries where atomic size may be more important than chemistry.

Iodine must have been dead, or at least partially decayed, when isotopic closure occurred for the trapped component. This is because, for simultaneous closure of iodine host and trapped component, addition of ^{128*}Xe from neutron capture and ^{129*}Xe from ^{129}I decay would displace the modified trapped component along the isochron and thus it would not be observable as anomalous. Therefore, closure would have had to occur after decay of at least some of the iodine, a model that can be tested to some extent by the data.

In Table 2 (columns 6 and 7), we compute two different inferred compositions for the trapped components of each

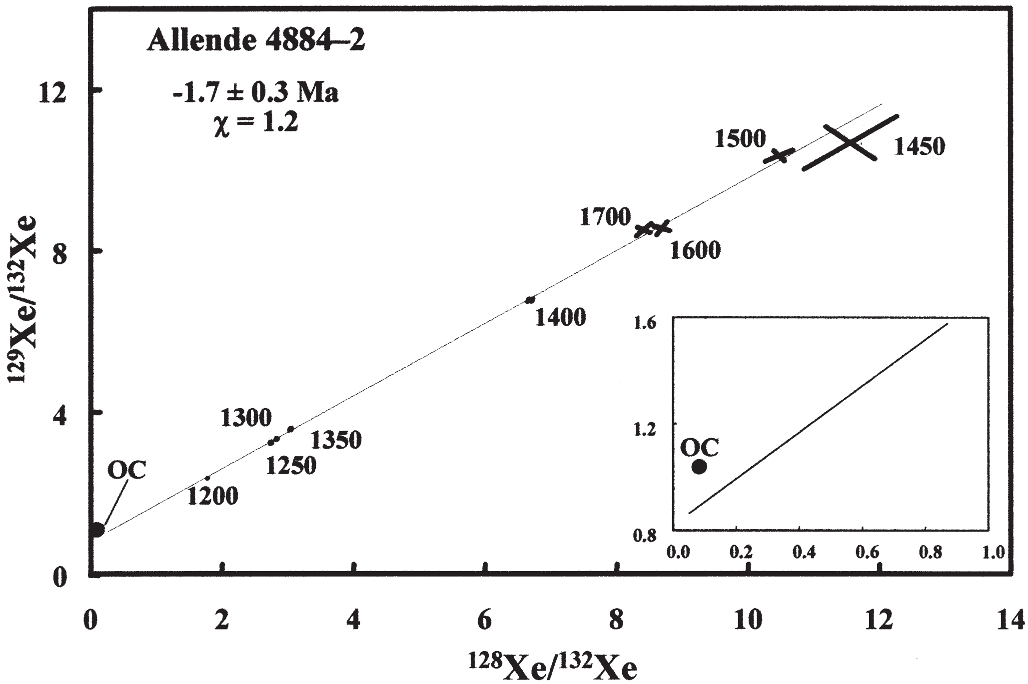

Fig. 4. I-Xe isochron plot for Allende DI 4884-2, defined by nine consecutive temperature fractions. The iodine host phase of this sample closed 1.7 ± 0.3 Ma before Shallowater, and requires one of the most "subplanetary" trapped Xe compositions of these dark inclusions (Table 2).

sample by alternately assuming a planetary ^{128}Xe/^{132}Xe ratio and a planetary ^{129}Xe/^{132}Xe ratio. The uncertainties of these inferred trapped Xe compositions are small (less than 1% in most cases) but, of course, do depend upon the assumption of normal planetary Xe for the other isotope ratio. Figure 7 shows the inferred values for the trapped ^{129}Xe/^{132}Xe ratios (assuming a planetary ^{128}Xe/^{132}Xe ratio) vs. I-Xe age (relative to Shallowater), demonstrating a trend of decreasing apparent (^{129}Xe/^{132}Xe)$_t$ with age. Two of these samples are part of the same inclusion, and all are from Allende, so the composition of trapped Xe cannot be a function of position in the solar nebula, as suggested by Ozima et al. (2002). The occurrence of different trapped components for samples of the same age, sometimes in the same inclusion, suggests that the correlation with age is not in itself strictly meaningful, and the negative extrap-

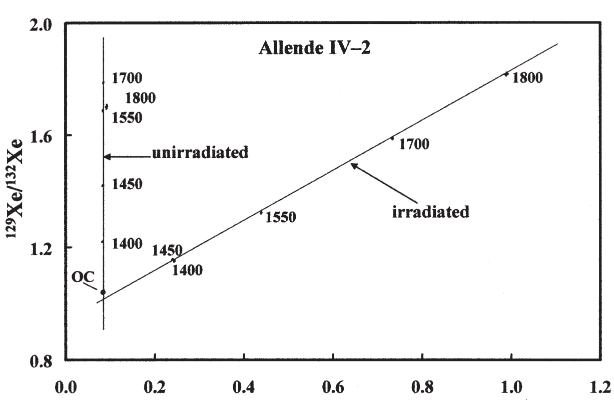

Fig. 5. Three-isotope correlation plots of both irradiated and unirradiated samples of Allende DI IV-2. The irradiated sample provides the I-Xe isochron, while both define mixing lines between iodine-derived and trapped components. Trapped Xe should lie at the intersection of the two lines, which would imply a normal planetary ^{128}Xe/^{132}Xe ratio and a (^{129}Xe/^{132}Xe)$_t$ that is significantly below planetary. However, such a "subplanetary" value for (^{129}Xe/^{132}Xe)$_t$ is not viable. The pseudo trapped component for the irradiated sample requires n-capture ^{128*}Xe, displacing it to the right from OC (see text).

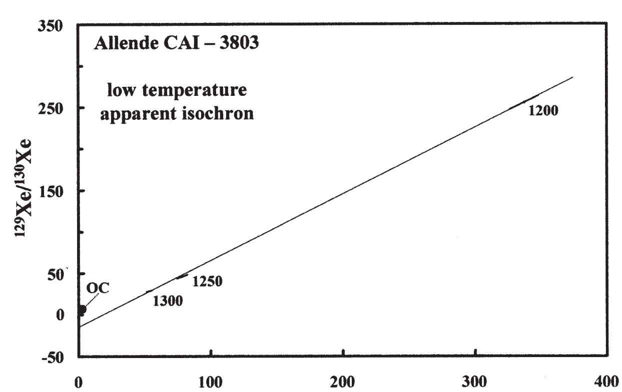

Fig. 6. I-Xe isochron plot for the Allende CAI-3803 (Pravdivtseva et al., 2003c). Here ^{129}Xe and ^{128}Xe are plotted vs. ^{130}Xe due to the presence of significant amounts of fission Xe. While three points do not generally define a convincing line, the small uncertainties and the co-linear nature suggest valid two-component mixing and an apparent isochron that requires a negative value for the trapped ^{129}Xe/^{130}Xe composition, if the ^{128}Xe/^{130}Xe ratio has the normal planetary value given by OC-Xe (0.511).

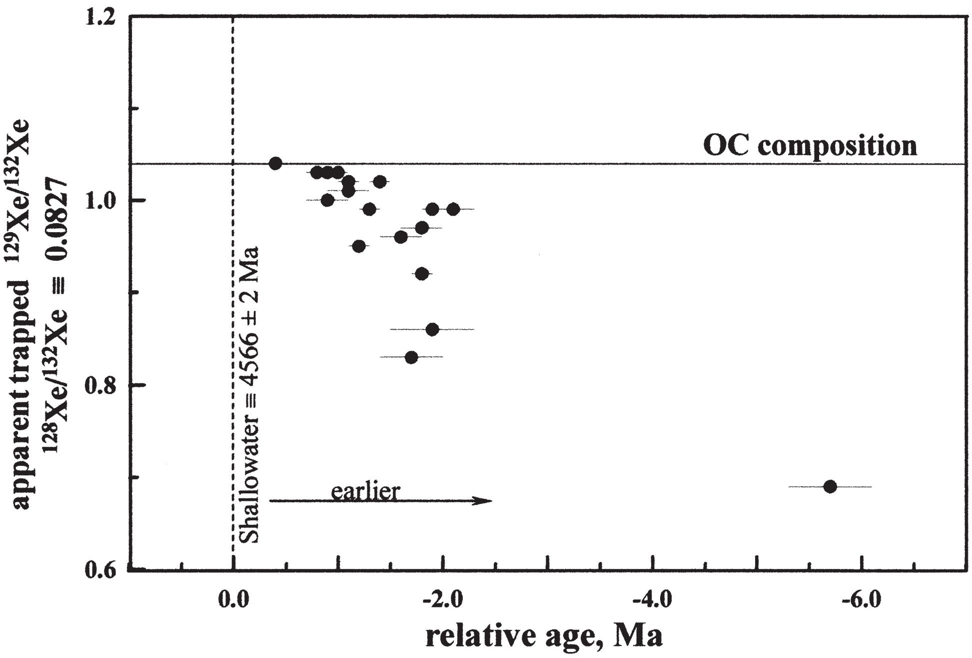

Fig. 7. Correlation between the apparent $^{129}Xe/^{132}Xe$ ratios in the trapped component and the relative I-Xe ages for the 18 Allende dark inclusions. These $(^{129}Xe/^{132}Xe)_t$ values are computed from the isochrons by setting the $(^{128}Xe/^{132}Xe)_t$ ratio equal to the normal planetary value given by OC-Xe (0.0827). The apparent trend observed here, lower apparent $(^{129}Xe/^{132}Xe)_t$ ratios for older I-Xe ages, would be expected if the trapped Xe is a pseudo component which includes some iodine-produced $^{128*}Xe$ (see Fig. 8 and text).

olated value (not shown) suggests interpretation of these $^{129}Xe/^{132}Xe$ ratios as real trapped components is most probably incorrect. However, such apparent trends would be expected if these trapped components were produced as we have proposed above. Figure 8 shows that incorporation of dead iodine (all of the ^{129}I decayed) with trapped Xe would produce an apparent trend of inferred trapped $^{129}Xe/^{132}Xe$ with age, in agreement with Figure 7. If true, this would place rigid constraints on the time when closure of the trapped component took place, but to refine this model, we need to know if the ^{129}I had totally or only partially decayed.

Figure 9 shows a different trend, using the alternate assumption: The apparent $(^{128}Xe/^{132}Xe)_t$ is computed from the isochron by using the planetary value for the $^{129}Xe/^{132}Xe$ ratio (Table 2, column 7), and plotted vs. the relative I-Xe age. For dead iodine $(^{128}Xe/^{132}Xe)_t$ is a superposition of trapped Xe and $^{128*}Xe$ from neutron capture, forming a pseudo trapped component. In this figure, we see a trend of increasing $(^{128}Xe/^{132}Xe)_t$ with age, opposite to that observed for $(^{129}Xe/^{132}Xe)_t$ in Figure 7. If the iodine were totally dead, the inferred $(^{128}Xe/^{132}Xe)_t$ ratio in this pseudo component would be dependent solely upon the ratio of Xe to iodine in the mixture, a plausibly random ratio, not one systematically increasing with antiquity (Fig. 9). However, such a trend would be expected if some live ^{129}I still existed at the time of trapped component closure.

Figure 10 shows the inferred value of $(^{128}Xe/^{132}Xe)_t$ in the pseudo trapped component for *partially* decayed ^{129}I in the iodine-Xe mixture at closure. In the case schematically shown, closure occurred ~10 Ma after precipitation of the iodine host phase (given by the slope of the dashed line). Also shown on the figure are the locations of the pseudo trapped component for totally dead iodine and that for simultaneous closure of the trapped component and the iodine host mineral. The values inferred for $(^{128}Xe/^{132}Xe)_t$ in Figure 10 for partially dead iodine are time ordered, similar to the trend observed in Figure 9. This suggests that the apparent trapped Xe in these aqueously altered inclusions is really a pseudo component, caused by an intimate mixture of planetary Xe (Q-Xe) and iodine whose ^{129}I had partially, but not totally decayed. The value of $^{129}I/^{127}I$ at the time of incorporation with planetary Xe (and closure) was less than the value at the time of closure of the primary iodine host (I-Xe age).

The highest position the pseudo trapped Xe can have on the isochron is constrained by the lowest data point on the isochron. Therefore, the minimum interval between closure of the iodine host (typically 1.5 Ma before Shallowater, or ~4.5675 Ga) and isolation of the pseudo trapped component (iodine-mixture) is set by the difference in the slopes of the isochron itself and a line defined by planetary trapped Xe (OC-Xe) and the lowest data point on the isochron (dashed line in Fig. 10). While one sample (Allende DI 4301-1) suggests a time interval of 21 Ma, a group of four Allende DIs cluster at ~13 Ma. Deferring to the latter group, we infer that a period ≥13 Ma must have elapsed between precipitation of the iodine host phase and isolation of pseudo trapped Xe.

The trends of Figures 7 and 9 are presumably visible because the nominal values for the iodine/Xe ratios are similar in these Allende DIs. These are only trends, and the scatter in these figures indicates considerable variability in this ratio. The isochrons for a few samples pass through or quite near OC, others require more "subplanetary" trapped Xe and still others require multiple values in a single sample (e.g., the multiple trapped components in Efremovka E80 and Allende IV-2 in the low-

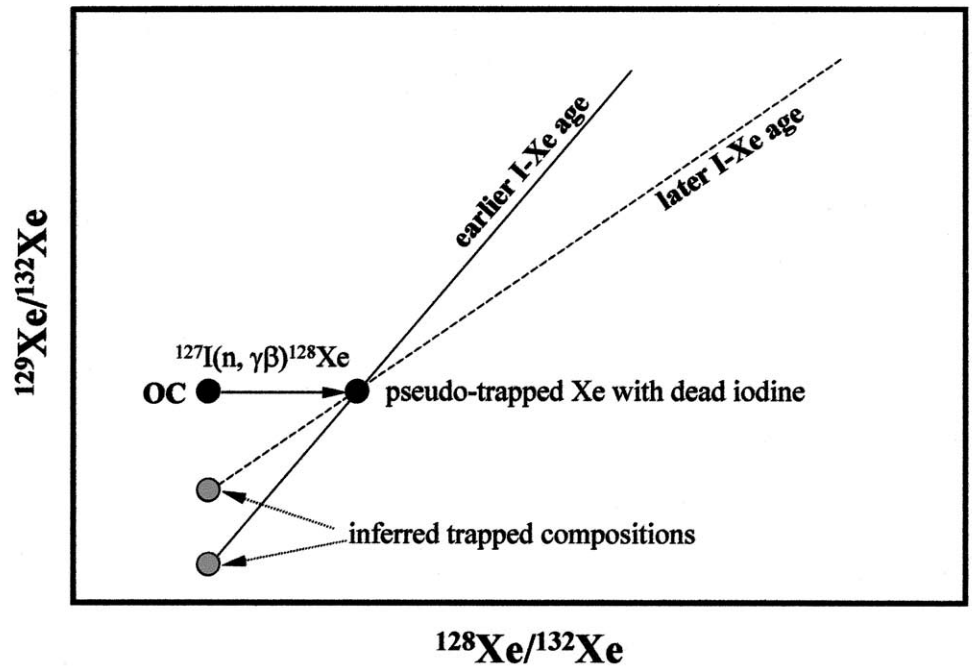

Fig. 8. If, on the average, all Allende DIs had the same ratio of iodine to xenon, they would have the same ratio of $^{128*}Xe$, to trapped Xe after irradiation and, on the average, the same pseudo trapped component (shown). Interpreting the apparent trapped composition in the conventional way (by setting $(^{128}Xe/^{132}Xe)_t$ equal to OC-Xe), the older samples with steeper isochrons would tend to have lower inferred $(^{129}Xe/^{132}Xe)_t$ values, the trend that is observed in Figure 7.

and high-temperature isochrons). This scatter may reflect different mixtures of surface and grain boundary sites, where iodine and Xe might be similarly trapped, and lattice sites which might favor one or the other.

4. I-Xe AGES

Figure 11 shows the I-Xe ages, relative to Shallowater, for all of the Allende components studied (CAIs [Pravdivtseva et al., 2003c], chondrules [Swindle et al., 1983], and DIs [Swindle et al., 1998; Krot et al., 1999; Pravdivtseva et al., 2003c]). The first I-Xe data for the Allende DIs (4301-1, 4314-3, IV-I, IV-2), combined with petrographic observations, lead us to conclude that the DIs experienced at least two-stage alteration: DIs whose I-Xe ages (from 0.8 to 1.9 Ma older than Shallowater) provide the closure time for the I-Xe system during the first alteration event. The second stage of alteration resulted in mobilization of Ca from the DIs and its redeposition as Ca-rich rims around the DIs and probably took place ~4.5 Ma later, as reflected by the I-Xe ages of the Allende CAIs (Pravdivtseva et al., 2003c). I-Xe ages of 18 Allende DIs reported here provide concordant I-Xe ages, refining the time for the first stage of alteration to ~1.6 Ma before Shallowater (4567.6 Ma), and the span of these alteration events to at least 5 Ma by their I-Xe ages alone.

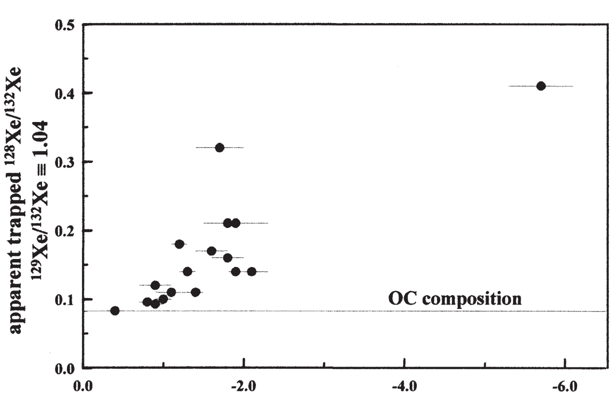

Fig. 9. Correlation between the apparent $(^{128}Xe/^{132}Xe)_t$ values and the relative I-Xe ages for the 18 Allende dark inclusions. Here the $(^{128}Xe/^{132}Xe)_t$ values are computed from the isochrons by setting the $(^{129}Xe/^{132}Xe)_t$ values to that of planetary, given by OC-Xe (1.04). The observed trend suggests systematically higher apparent $(^{128}Xe/^{132}Xe)_t$ ratios with older I-Xe ages. This trend would be expected if the pseudo trapped Xe is a normal planetary Xe accompanied by both iodine-produced $^{128*}Xe$ and some radiogenic $^{129*}Xe$ (see Fig. 10 and text).

Previously reported I-Xe ages of Efremovka DIs E53 and E39 (Krot et al., 1999) correlate with their degrees of alteration and O-isotopic compositions, with least altered E53 being the oldest. DI E80 reported in this work shows the highest degree of replacement of primary minerals by secondary phases among Efremovka DIs. The I-Xe age of E80 is concordant with the age of E39 (Krot et al., 1999) and indicates that this sample was altered either later, or underwent longer alteration than E53. DIs LV1 and E80 are mineralogicaly similar (Brearley, 1998; Krot et al., 1999). In contrast with other CV3 DIs, LV2 shows little evidence of aqueous alteration. It has an apparent isochron age younger than LV1 and abundant trapped Xe. Vigarano DI 2226 is composed of high- and low-Ca pyroxene and olivine fragments set in a fine-grained matrix with bands of densely packed, fine-grained matrix-like material, interpreted

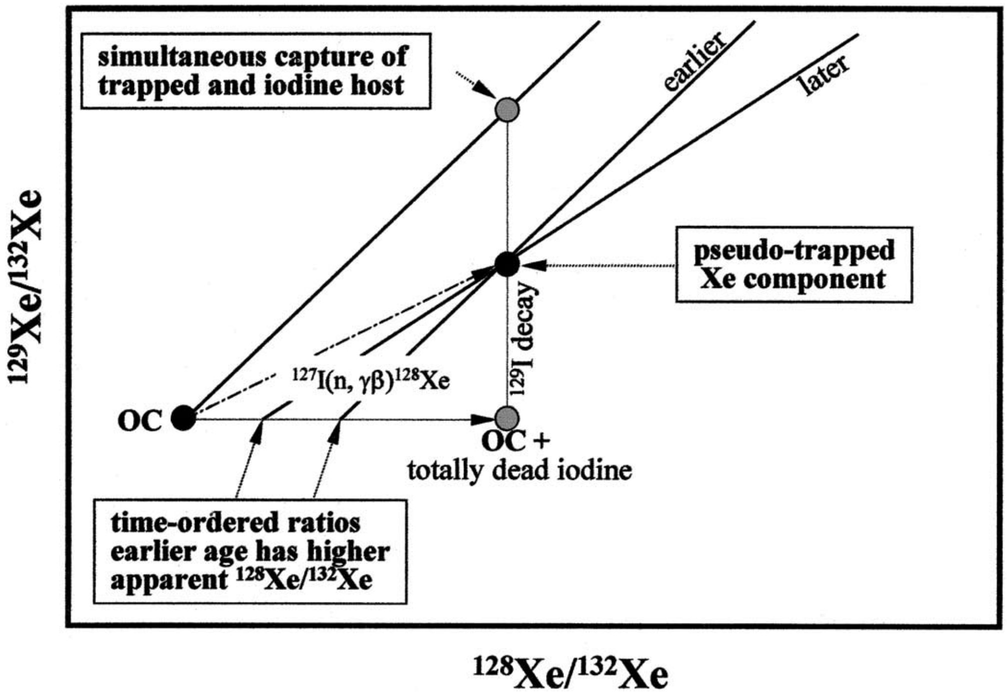

Fig. 10. Three potential locations for the pseudo trapped Xe component. If the trapped component were an intimate mixture of iodine and Xe, and it closed simultaneously with the iodine host phase (presumably sodalite), the apparent trapped component would lie along the isochron and would not be observed as anomalous. If the iodine were completely dead, the apparent trapped composition would lie on a horizontal line to the right of OC. In this case, no systematic (time-ordered) trend of apparent $(^{128}Xe/^{132}Xe)_t$ values would be observed (they would define the same value for a fixed iodine/Xe ratio, and vary randomly for a randomly variable ratio). However, if the pseudo trapped component contains both iodine-produced ^{128*}Xe, from the irradiation, and some radiogenic ^{129*}Xe, it would plot (on the average) as shown schematically and provide time-ordered values for the apparent $(^{128}Xe/^{132}Xe)_t$ ratios, as indicated, consistent with the trend observed in Figure 9. Shown is hypothetical closure of pseudo trapped Xe ~10 Ma after closure of the iodine host phase, a time interval given by the relative slopes of the isochron and the dashed line. The shortest delay time is set by the lowest data point on the isochrons, corresponding to $\Delta t \geq 13$ Ma (see text).

to be products of sedimentary processes (Tomeoka and Kojima, 1998). The I-Xe age of DI 2226 is 8.8 ± 0.6 Ma younger than Shallowater. All together the I-Xe ages of these 22 DIs from the oxidized and reduced CV3 meteorites span ~15 Ma, suggesting a long period of low temperature alteration (Pravdivtseva et al., 2003b).

The fact that pseudo trapped Xe in the DIs, in the model we propose, seems to require emplacement some 13 Ma or so after the earliest precipitation of an iodine host phase supports the conclusion that the duration of alteration processes in CV3 meteorites may well be much longer than previously believed.

5. CONCLUSIONS

The I-Xe isochrons for most of the DIs from Allende, Efremovka, Vigarano, and Leoville studied here are excellent two-component mixing lines between trapped and iodine-derived components. The uncertainties of slopes are small, providing I-Xe ages of high precision. The surprising observation is that the isochrons for most of these samples pass significantly below the uniformly acknowledged composition of planetary Xe (OC or Q), requiring "subplanetary" trapped components (either a ^{129}Xe/^{132}Xe ratio significantly below planetary, or a ^{128}Xe/^{132}Xe ratio significantly above planetary). Analysis of irradiated and unirradiated samples of Allende DI IV-2 proves that the ^{128}Xe/^{132}Xe ratio in the trapped component of the unirradiated sample is of normal planetary composition, suggesting that the ^{129}Xe/^{132}Xe ratio must be below planetary. However, planetary Xe is uniform and well characterized. The ^{129}Xe/^{132}Xe ratio cannot be significantly modified by open system ^{129}I decay, so the planetary ^{129}Xe/^{132}Xe ratio could never have been significantly below its present nominal value. Therefore, "subplanetary" trapped Xe must be a pseudo trapped component, one that varies from sample to sample and cannot be formed by mixtures of planetary Xe with any known Xe component.

We conclude that ^{128*}Xe, produced from stable ^{127}I by the irradiations, is responsible for the "subplanetary" nature of the trapped Xe, a conclusion consistent with the observations of Gilmour et al. (2001). The trends displayed in the inferred ^{128}Xe/^{132}Xe and ^{129}Xe/^{132}Xe ratios vs. I-Xe age (Figs. 7 and 9), however, suggest that not all of the ^{129}I had decayed at the time of trapped Xe-I incorporation. It would thus appear that this pseudo trapped component was emplaced ≥13 Ma after formation of the iodine host phase (Fig. 10), a conclusion that seems qualitatively consistent with the extended period of aqueous activity apparent in Figures 1 and 11.

The iodine host phase precipitated during the first period of postformational aqueous activity (Krot et al., 2002; Pravdivt-

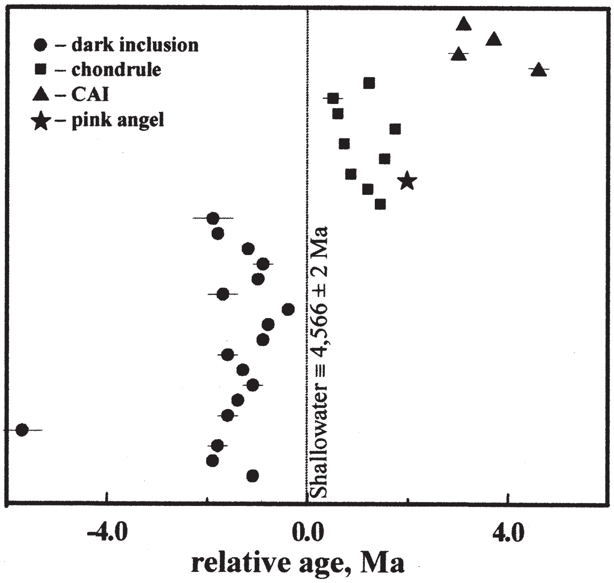

Fig. 11. Relative I-Xe ages of different Allende components. Dark inclusions cluster tightly (with one exception) at –1.6 Ma (older than Shallowater), the chondrules and the Pink Angel are intermediate, ~1.6 Ma after Shallowater (Swindle et al., 1983, 1988) and the CAIs are the youngest, ~3.5 Ma after Shallowater (Pravdivtseva et al., 2003c). This wide span suggests multiple episodes of aqueous alteration (Krot et al., 2002; Pravdivtseva et al., 2003c), or an extended duration for aqueous activity. The pseudo trapped Xe inferred in this work is consistent with these conclusions, extending this to the ~15 Ma as suggested by the I-Xe ages for DIs from the reduced CV3s (Fig. 1).

seva et al., 2003c), at the time indicated by the I-Xe ages of these dark inclusions. Later incorporation of planetary Xe and residual iodine defined the trapped component of these inclusions. Whether this occurred by adsorption on surfaces (Wacker, 1989; Hohenberg et al., 2002), as is perhaps indicated for phase-Q, or by implantation onto surfaces by shock (Caffee et al., 1982; Gilmour et al., 2001), the subsequent neutron irradiation utilized for I-Xe dating produces a pseudo trapped Xe component with elevated ^{128}Xe. Incorporation of this pseudo trapped component must have occurred after formation of the iodine host phase because ^{129*}Xe from decay of the full complement of ^{129}I would have produced a pseudo trapped component on the isochron (as would any fraction with the same initial ^{129}I/^{127}I ratio) and "subplanetary" trapped Xe would never have been detected.

Acknowledgments—We kindly acknowledge Sasha Krot for all 22 of these DIs, and for many helpful discussions. We thank the University of Missouri and the personnel at the University of Missouri Research Reactor, for the neutrons irradiations that made this work possible. We thank Tim Swindle, Kurt Marti, James Whitby, and associate editor Uli Ott for many helpful discussions. This work was supported, in part, by NASA Grant NAG5-12776.

Associate editor: U. Ott

REFERENCES

Anders E. and Grevesse N. (1989) Abundances of the elements: Meteoritic and solar. *Geochim. Cosmochim. Acta* **53,** 197–214.

Bischoff A., Palme H., Spettel B., Clayton R. N., and Mayeda T. K. (1988) The chemical composition of dark inclusions from the Allende meteorite. *Lunar Planet. Sci. XIX*, 88–89 (abstr.).

Brearley A. J (1998) Dark inclusions in the Leoville CV3 carbonaceous chondrite. *Lunar Planet. Sci. XXIX*. Lunar Planet. Inst., Houston, #1245 (abstr.).

Buchanan P. C., Zolensky M. E., and Reid A. M. (1997) Petrology of Allende dark inclusions. *Geochim. Cosmochim. Acta* **61,** 1733–1743.

Caffee M. W., Hohenberg C. M., Hörz F., Hudson B., Kennedy B. M., Podosek F. A., and Swindle T. D. (1982) Shock disturbance of the I-Xe system. *Proc. Lunar Planet. Sci. Conf. 13, J. Geophys. Res. Suppl.* **87,** A318–A330.

Drozd R. J. and Podosek F. A. (1976) Primordial ^{129}Xe in meteorites. *Earth Planet. Sci. Lett.* **31,** 15–30.

Fruland R. M., King E. A., and McKay D. S. (1978) Allende dark inclusions. *Proc. Lunar Sci. Conf.* **9,** 1305–1329.

Gilmour J. D. and Saxton J. M. (2001). A time-scale of formation of the first solids. *Phil. Trans. Roy. Soc. Lond.* A359, 2037–2048.

Gilmour J. D., Whitby J. A., and Turner G. (2001) Negative correlation of iodine-129/iodine-127 and xenon-129/xenon-132: Product of closed-system evolution or evidence of a mixed component. *Meteorit. Planet. Sci.* **36,** 1283–1286.

Hohenberg C. M. (1980) High sensitivity pulse-counting mass spectrometer system for noble gas analysis. *Rev. Sci. Instrum.* **51,** 1075–1082.

Hohenberg C. M. and Reynolds J. H. (1969) Preservation of the iodine-xenon record in meteorites. *J. Geophys. Res.* **74,** 6679–6683.

Hohenberg C. M., Pravdivtseva O., and Meshik A. (2000). Reexamination of anomalous I-Xe ages: Orgueil and Murchison magnetites and Allegan feldspar. *Geochim. Cosmochim. Acta* **64,** 4257–4262.

Hohenberg C. M. Thonnard N., and Meshik A. (2002). Active capture and anomalous adsorption: New mechanisms for the incorporation of heavy noble gases. *Meteorit. Planet. Sci.* **37,** 257–267.

Huss G. R., Lewis R. S., and Hemkin S. (1996) The "normal planetary" noble gas component in primitive chondrites: Compositions, carrier and metamorphic history. *Geochim. Cosmochim. Acta* **60,** 3311–3340.

Johnson C. A., Prinz M., Weisberg M. K., Clayton R. N., and Mayeda T. K. (1990) Dark inclusions in Allende, Leoville, and Vigarano: Evidence for nebular oxidation of CV3 constituents. *Geochim. Cosmochim. Acta* **54,** 819–830.

Kennedy B. M (1981) Potassium-argon and iodine-xenon gas retention ages of enstatite chondrite meteorites. Ph.D. thesis, Washington University, St. Louis.

Kennedy B. M., Hudson B., Hohenberg C. M., and Podosek F. A. (1988) ^{129}I/^{127}I variations among enstatite chondrites. *Geochim. Cosmochim. Acta* **52,** 101–111.

Kojima T. and Tomeoka K. (1996) Indicators of aqueous alteration and thermal metamorphism on the CV parent body: Microtextures of a dark inclusion from Allende. *Geochim. Cosmochim. Acta* **60,** 2651–2666.

Kojima T., Tomeoka K., and Takeda H. (1993) Unusual dark clasts in the Vigarano CV3 carbonaceous chondrite: Record of parent body process. *Meteorit. Planet. Sci.* **28,** 649–658.

Kracher A., Keil K., Kallemeyn G. W., Wasson J. T., Clayton R. N., and Huss G. I. (1985) The Leoville (CV3) accretionary breccia. *Proc. XVI Lunar Planet. Sci. Conf.*, D123–D135.

Krot A. N., Petaev M. I., Scott E. R. D., Choi B.-G., Zolensky M. E., and Keil K. (1998a) Progressive alteration in CV3 chondrites: More evidence for asteroidal alteration. *Meteorit. Planet. Sci.* **33,** 1065–1085.

Krot A. N., Petaev M. I., Zolensky M. E., Keil K., Scott E. R. D., and Nakamura K. (1998b) Secondary calcium-iron-rich minerals in the Bali-like and Allende-like oxidized CV3 chondrites and Allende dark inclusions. *Meteorit. Planet. Sci.* **33,** 623–645.

Krot A. N., Brearley A. J., Ulyanov A. A., Biryukov V. V., Swindle T. D., Keil K., Mittlefehldt D. W., Scott E. R. D., Clayton R. N., and Mayeda T. K. (1999) Mineralogy, petrography, bulk chemical, iodine-xenon, and oxygen-isotopic compositions of dark inclusions in the reduced CV3 chondrite Efremovka. *Meteorit. Planet. Sci.* **34,** 67–89.

Krot A. N., Hohenberg C. M., Meshik A. P., Pravdivtseva O. V., Hiyagon H., Petaev M. I., Weisberg M. K., Meibom A., and Keil K.

(2002). Two-stage asteroidal alteration of the Allende dark inclusions. *Meteorit. Planet. Sci.* **37,** A82.

Kurat G., Palme H., Brandstätter F, and Huth J. (1989) Allende xenolith AF: Undisturbed record of condensation and aggregation of matter in the solar nebula. *Z. Naturforsch.* 44a, 988–1004.

Lavielle B. and Marti K. (1992) Trapped xenon in ordinary chondrites. *J. Geophys. Res.* **97,** 20875–20881.

Lewis R. S., Srinivasan B., and Anders E. (1975) Host phase of a strange xenon component in Allende. *Science* **190,** 1251–1262.

Marti K. (1967) Trapped xenon and the classification of chondrites. *Earth Planet. Sci. Lett.* **2,** 193–196.

Nichols R. H. Jr., Hohenberg C. M., Kehm K., Kim Y., and Marti K. (1994) I-Xe studies of the Acapulco meteorite: Absolute I-Xe ages of individual phosphate grains and the Bjurböle standard. *Geochim. Cosmochim. Acta* **58,** 2553–2561.

Ott U. (2002). Noble gases in meteorites—trapped components. In *Reviews in Mineralogy and Geochemistry*, **47** (eds. D. Porcelli, C. J. Ballentine, and R. Wieler), pp. 71–100. Mineralog. Soc. of America Press, Washington, DC.

Ott U., Mack R., and Chang S. (1981) Noble-gas-rich separates from the Allende meteorite. *Geochim. Cosmochim. Acta* **45,** 1751–1788.

Ozima M., Miura Y. N., and Podosek F. A. (2002) Revisiting I-Xe systematics, an early solar system chronometer. 12th Ann. Goldschmidt Conf. *Geochim. Cosmochim. Acta* **66,** A576.

Palme H., Kurat G., Spettel B., and Burghele A. (1989) Chemical composition of an unusual xenolith of the Allende meteorite. *Z. Naturforsch.* 44a, 1005–1014.

Pepin R. O. and Signer P. (1965) Primordial rare gases in meteorites. *Science* **149,** 253–265.

Pepin R. O., Becker R. H., and Rider P. E. (1995) Xenon and krypton isotopes in extraterrestrial regolith soils and in the solar wind. *Geochim. Cosmochim. Acta* **59,** 4997–5022.

Pravdivtseva O. V., Hohenberg C. M., and Meshik A. P. (2003a) The I-Xe age of Orgueil magnetite: New results. *Lunar Planet. Sci. XXXIV.* Lunar Planet. Inst., Houston, #1863 (abstr.).

Pravdivtseva O. V., Hohenberg C. M., Meshik A. P., Krot A. N., and Brearley A. J. (2003b) I-Xe ages of the dark inclusions from the reduced CV3 chondrites Leoville, Efremovka, and Vigarano. *Meteorit. Planet. Sci.* **38,** A140.

Pravdivtseva O. V., Krot A. N., Hohenberg C. M., Meshik A. P., Weisberg M. K., and Keil K. (2003c) The I-Xe record of alteration in the Allende CV chondrite. *Geochim. Cosmochim. Acta* **67,** 5011–5026.

Reynolds J. H. (1960) Determination of the age of the elements. *Phys. Rev. Lett.* **4,** 8–10.

Reynolds J. H., Frick U., Neil J. M., and Phinney D. L. (1978) Rare-gas-rich separates from carbonaceous chondrites. *Geochim. Cosmochim. Acta* **42,** 1775–1797.

Signer P, Suess H. E (1963) Rare gases in the sun, in the atmosphere and in meteorites. *Earth Sciences and Meteoritics,* North Holland, Amsterdam, 241.

Swindle T. D. (1998) Implications of iodine-xenon studies for the timing and location of secondary alteration. *Meteorit. Planet. Sci.* **33,** 1147–1155.

Swindle T. D. and Podosek F. A. (1988) Iodine-xenon dating. In *Meteorites and the Early Solar System* (eds. J. F. Kerridge and M. S. Matthews), pp. 1127–1146. University of Arizona Press, Tucson.

Swindle T. D., Caffee M. W., Hohenberg C. M., and Lindstrom M. M. (1983) I-Xe studies of individual Allende chondrules. *Geochim. Cosmochim. Acta* **47,** 2157–2177.

Swindle T. D., Caffee M. W., and Hohenberg C. M. (1988) Iodine-xenon studies of Allende inclusions: Eggs and the Pink Angel. *Geochim. Cosmochim. Acta* **52,** 2215–2227.

Swindle T. D., Cohen B., Li B., Olson E., Krot A. N., Birjukov V. V., and Ulyanov A. A. (1998) Iodine-xenon studies of separated components of the Efremovka (CV3) meteorite. *Lunar Planet. Sci. XXIX.* Lunar Planet. Inst., Houston, #1005 (abstr.).

Tomeoka K. and Kojima T. (1998) Arcuate band texture in a dark inclusion from the Vigarano CV3 chondrite: Possible evidence for early sedimentary processes. *Meteorit. Planet. Sci.* **33,** 519–525.

Wacker J. F. (1989) Laboratory simulation of meteoritic noble gases. III. Sorption of neon, argon, krypton, and xenon on carbon: Elemental fractionation. *Geochim. Cosmochim. Acta* **53,** 1421–1433.

Weisberg M. K, Prinz M (1997) Fayalitic olivine in CV3 chondrite matrix and dark inclusions: A nebular origin. In *Workshop on Parent-Body and Nebular Modification of Chondritic Materials* (eds. M. E. Zolensky, A. N. Krot, and E. R. D. Scott), pp. 66–67. LPI Tech. Rept. No. **97–02,** Part 1, Lunar Planet. Inst., Houston, Texas.

Weisberg M. K., Prinz M., Boesenberg S., Kozhushko G., Clayton R. N., Mayeda T. K., and Ebihara M. E. (1996) A petrologic and oxygen isotopic study of six Allende dark inclusions: Evaluation of nebular vs. asteroidal models for their origin. *Lunar Planet Sci. XXVII,* 1407–1408 (abstr.).